

APPENDIX C

HYDROLOGIC, HYDRAULIC, AND SEDIMENT TRANSPORT MODELING

Contents

| | <i>Page</i> |
|---|-------------|
| C.1 Hydrology | C-1 |
| C.1.1 Historical Flows Prior to 2009 | C-2 |
| C.1.2 Simulated Flows under SJRRP | C-5 |
| C.2 Sediment Transport and Geomorphic Context | C-11 |
| C.2.1 Historical Aerial Photography | C-11 |
| C.2.2 Measured Sediment Loads | C-12 |
| C.2.2.1 Bed Load | C-13 |
| C.2.2.2 Suspended Load | C-13 |
| C.2.3 Estimated Sediment Budget | C-13 |
| C.2.3.1 SKB to GRF (RM 232.1 to 227.6) | C-13 |
| C.2.3.2 GRF to Lower 2A (RM 227.6 to 219.3) | C-14 |
| C.2.3.3 Lower 2A to SJB (RM 219.3 to 216.0) | C-14 |
| C.2.3.4 SJB to MEN (RM 219.3 to 202.1) | C-19 |
| C.2.4 Bed Material | C-19 |
| C.5 Hydraulic Modeling | C-21 |
| C.6 Sediment Modeling | C-21 |
| C.6.1 Sediment Transport Capacity | C-23 |
| C.6.2 Engelund and Hansen's Method | C-23 |
| C.6.3 Laursen's Formula and Modified Version | C-24 |
| C.6.4 Wu, et al. | C-25 |
| C.6.5 Parker's Method | C-26 |
| C.6.6 Results | C-27 |
| C.7 Option 1 | C-29 |
| C.7.1 Bed Elevations | C-29 |
| C.7.2 Sediment Loads | C-30 |
| C.7.3 Water Surface Profiles | C-30 |
| C.8 Option 2 | C-31 |
| C.8.1 Channel Bed Elevations | C-31 |
| C.8.2 Sediment Loads | C-32 |
| C.8.3 Water Surface Elevations | C-32 |
| C.9 Impacts to Floodplain Habitat in Reach 2B | C-44 |
| C.9.1 Previous Estimate | C-44 |
| C.9.2 Inundation under Option 2 | C-47 |
| C.9.2.1 Geometry | C-47 |
| C.9.2.2 Roughness | C-54 |
| C.9.2.3 Boundary Conditions | C-54 |
| C.9.2.4 Results | C-55 |
| C.10 Impacts to Flood Conveyance in Reach 3 | C-60 |

Figures

| | |
|--|------|
| Figure C-1.—Map of stream gages and sediment measurement locations within Reaches 1 to 3..... | C-3 |
| Figure C-2.—Monthly flow duration at GRF located in Reach 2A for WY 2000 through 2007. | C-4 |
| Figure C-3.—Monthly flow duration at SJB in Reach 2B for WY 2000 through 2007. | C-4 |
| Figure C-4.—Monthly flow duration at MEN in Reach 3 for WY 2000 through 2007. | C-5 |
| Figure C-5.—San Joaquin River flows at upstream end of Reach 2 as reported in Exhibit B of the Stipulation of Settlement. | C-6 |
| Figure C-6.—San Joaquin River flows at upstream end of Reach 3 as reported in Exhibit B of the Stipulation of Settlement. | C-7 |
| Figure C-7.—Simulated monthly flow duration at GRF in Reach 2A under the SJRRP. | C-7 |
| Figure C-8.—Simulated monthly flow duration at SJB under the SJRRP. | C-8 |
| Figure C-9.—Simulated monthly flow duration at MEN in Reach 3 under the SJRRP. | C-8 |
| Figure C-10.—Simulated monthly flow duration at JBP under the SJRRP. | C-9 |
| Figure C-11.—Measured daily average flows at GRF, SJB, and MEN for WY 2010 through 2012. | C-9 |
| Figure C-12.—Simulated flows for WY 1986 under Restoration operations. .. | C-10 |
| Figure C-13.—Flows simulated by RiverWare at upstream end of Reach 2A for WY 1953 through 2002..... | C-11 |
| Figure C-14.—Measured suspended sediment concentration at SJB for WY 2010 through 2012. | C-15 |
| Figure C-15.—Measured gravel and sand bed load transport rate at SJB for WY 2010 - 2012..... | C-16 |
| Figure C-16.—Measured suspended sediment concentration MEN for WY 2010 - 2012..... | C-17 |
| Figure C-17.— Measured bed load on San Joaquin at MEN for WY 2010 - 2012..... | C-18 |
| Figure C-18.—Estimated annual total sand sediment loads in WY 2010 - 2012 for sediment measurement locations..... | C-19 |
| Figure C-19.—Average bed material gradations in San Joaquin River by RM. | C-20 |
| Figure C-20.—Cross section layout for Reaches 2B and 3 | C-22 |
| Figure C-21.—Comparison between Laursen’s function and fitted function.... | C-25 |

Figure C-22.—Comparison of transport formulas to measured sand load data at SJB.C-28

Figure C-23.—Comparison of transport formulas to measured sand load data at MEN.C-28

Figure C-24.—Initial and 25 year simulated thalweg elevation for Reach 2A through Reach 3.C-34

Figure C-25.—Initial and 25 year simulated thalweg elevation in vicinity of Compact Bypass.....C-35

Figure C-26.—Initial and 25 year simulated thalweg elevation in vicinity of Compact Bypass, with and without inflows from the Fresno Slough for Options 1 and 2.C-36

Figure C-27.—Simulated erosion in Reach 2B and deposition in Reach 3 within 50-yr period for Option 1 and 2 without subsidence.C-37

Figure C-28.—Simulated sediment loads within 50-yr period for Option 1 and 2 without subsidenceC-38

Figure C-29. Simulated sediment loads at upstream end of Reach 2B and downstream end of Reach 3 within 50-yr period for Option 1 and 2 without subsidence.....C-39

Figure C-30.—Thalweg elevation and water surface elevation at a flow of 1,200 cfs for Option 1 and 2 after a 25 year SRH-1D simulation without subsidence.....C-40

Figure C-31.—Thalweg elevation and water surface elevation at a flow of 4,500 cfs for Option 1 and 2 after a 25 year SRH-1D simulation without subsidence.....C-41

Figure C-32.—Thalweg elevation for Option 1 for various years after construction.C-42

Figure C-33.—Thalweg elevation for Option 2 for various years after construction.C-43

Figure C-34.—Habitat Suitability Index values as a function of depth and velocity from Stanislaus River (Aceituno, 1990).....C-45

Figure C-35.—Side channel in Reach 2A.....C-49

Figure C-36.—Examples of split/side flow channels and a backwater slough in Reach 2A at RM 221 to 220C-50

Figure C-37.—Reach 3 slough example in 1937 aerial photograph.....C-51

Figure C-38.—High flow channel and point bars in Reach 2B in 1937 aerial photograph.C-52

Figure C-39.—Examples of high flow channels in Reach 1B at RM 231 in 2011 aerial photograph.C-52

Figure C-40.—Floodplain grading assumed to estimate floodplain inundation for Option 2.....C-53

Figure C-41.—Area of inundation in Reach 2B at various flows assuming Option 2 and proposed levee alignment.....C-56

Figure C-42.—Depth of inundation for a flow of 1,200 cfs in Reach 2B
 under Option 2.C-57

Figure C-43.—Depth of inundation for a flow of 2180 cfs in Reach 2B
 under Option 2.C-58

Figure C-44.—Depth of inundation for a flow of 3,000 cfs in Reach 2B
 under Option 2.C-59

Figure C-45.—Maximum water surface elevations for a flow of 4500 cfs
 in Reach 3 downstream of Bypass.C-62

Tables

Table C-1.—Active Stream Gages Relevant to SJRRPC-1

Table C-2.—Return Period of Flow above a Given Level Based Upon
 Simulated Daily Average Flows from River WareC-10

Table C-3.—Historical Aerial Photography Used in the Floodplain DesignC-12

Table C-4.—Information Collected at Sampling Sites for WY2010 to 2012....C-12

Table C-5.—Summary of Bed Material Measurements in Reach 2 and 3.C-20

Table C-6.—Previous Estimated Inundated Area for FP2 and FP4 Levee
 Setbacks in Reach 2B Assuming Existing Bed Geometry.....C-44

Table C-7.—Cover HSI Scores Assumed in Reclamation.....C-46

Table C-8.—Estimates of Existing Inundation and Suitable Juvenile Salmon
 Rearing Habitat in the SJRRP Reaches C-46

Table C-9.—Assumed Roughness Values in SRH-2D for Reach 2B.C-54

Table C-10.—Downstream Boundary Condition Used in SRH-2D.....C-54

Table C-11.—Estimated Inundation in Reach 2B under Option 2.C-55

Table C-12.—Estimated Inundation in the Compact Bypass under Option 2...C-56

C Hydrologic, Hydraulic and Sediment Transport Modeling

This appendix summarizes the hydrologic, hydraulic, and sediment data and analysis used to support the design and analysis.

C.1 Hydrology

There is a network of stream gages in the San Joaquin basin downstream of Friant Dam (table C-1). The gage “San Joaquin River (SJR) at Gravelly Ford” (GRF) is located at the upstream end of Reach 2A and the gages within Reach 2B are SJR below Bifurcation (SJB) and San Joaquin River at San Mateo Road near Mendota (SJN). The flows in Reach 3 are recorded by SJR near Mendota, CA (MEN). The flows contributed by Fresno Slough into Mendota Pool are recorded by James Bypass (JBP).

Table C-1.—Active Stream Gages Relevant to SJRRP

| Name | ID | USGS ID | RM | Longitude | Latitude | Agency | Reach |
|---|-----|----------|-------|-------------|-----------|--------|-------|
| SJR release from Friant Dam | MIL | | 267.5 | -119.705000 | 37.001000 | USBR | 1A |
| Cottonwood Creek near Friant | CTK | | - | -119.696000 | 36.967000 | USBR | 1A |
| SJR below Friant, CA | SJF | 11251000 | 266 | -119.723300 | 36.984400 | USGS | 1A |
| Little Dry Creek near Friant | LDC | | - | -119.683000 | 36.942000 | USBR | 1A |
| SJR at Hwy 41 | H41 | 11252275 | 255.1 | -119.792127 | 36.876182 | USBR | 1B |
| SJR at Donny Bridge | DYB | | 240.7 | -119.965800 | 36.833500 | USBR | 1B |
| SJR at Hwy 145 Skaggs Bridge | SKB | 11252975 | 232.1 | -120.056200 | 36.822800 | USBR | 1B |
| SJR at Gravelly Ford | GRF | 11253058 | 227.6 | -120.160000 | 36.798000 | USBR | 2A |
| SJR below Bifurcation | SJB | 11253115 | 216 | -120.286000 | 36.773000 | USBR | 2B |
| SJR at San Mateo Road near Mendota | SJN | 11253130 | 211.8 | -120.306664 | 36.778889 | USGS | 2B |
| Chowchilla Bypass at Head | CBP | | - | -120.285000 | 36.774000 | USBR | C |
| Eastside Bypass near El Nido | ELN | | - | -120.605300 | 37.147500 | DWR | E |
| James Bypass (Fresno Slough) near San Joaquin, CA | JBP | 11253500 | - | -120.180300 | 36.652500 | USBR | 2B |
| SJR near Mendota, CA | MEN | 11254000 | 202.1 | -120.377200 | 36.810600 | USGS | 3 |
| SJR near Dos Palos, CA | SDP | 11256000 | 181.5 | -120.500000 | 36.995000 | USGS | 3 |

| Name | ID | USGS ID | RM | Longitude | Latitude | Agency | Reach |
|--------------------------|-----|---------|----|-------------|-----------|--------|-------|
| SJR near Washington Road | SWA | | - | -120.587000 | 37.115320 | DWR | 4A |

USBR: U.S. Bureau of Reclamation (Reclamation)

USGS: U.S. Geological Survey

ID: Identification

RM: River Mile

C.1.1 Historical Flows Prior to 2009

The flow duration curves for the recent measured historical flow before the implementation of the SJRRP (water year [WY] 2000 - 2007) in Reach 2A, Reach 2B, and Reach 3 are given in figure C-2, figure C-3, and figure C-4, respectively. Reach 2B was without flow the majority of the time and the 25 percent exceedance flow was 0 for all months except for April, May, and June, which corresponds to periods that there can be flood releases from Millerton Reservoir. The 50 percent exceedance flow was 0 for all months.

The maximum daily average flow that occurred during this period was on April 23, 2005, and was 1,755 cfs. The maximum daily average flow for the period of WY 1977 until WY 2007 was 2,660 cfs and occurred on May 23, 1978.

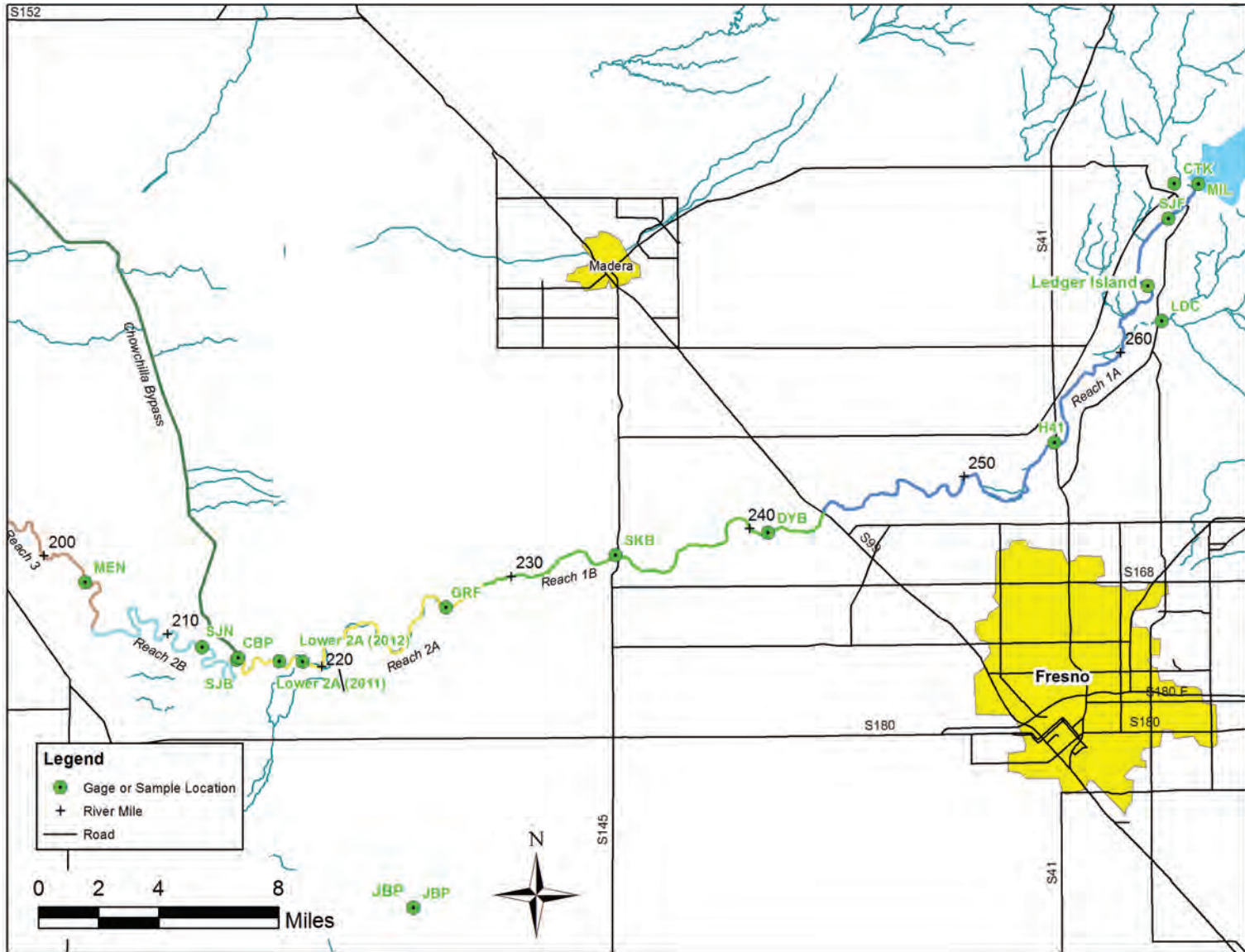


Figure C-1.—Map of stream gages and sediment measurement locations within Reaches 1 to 3.

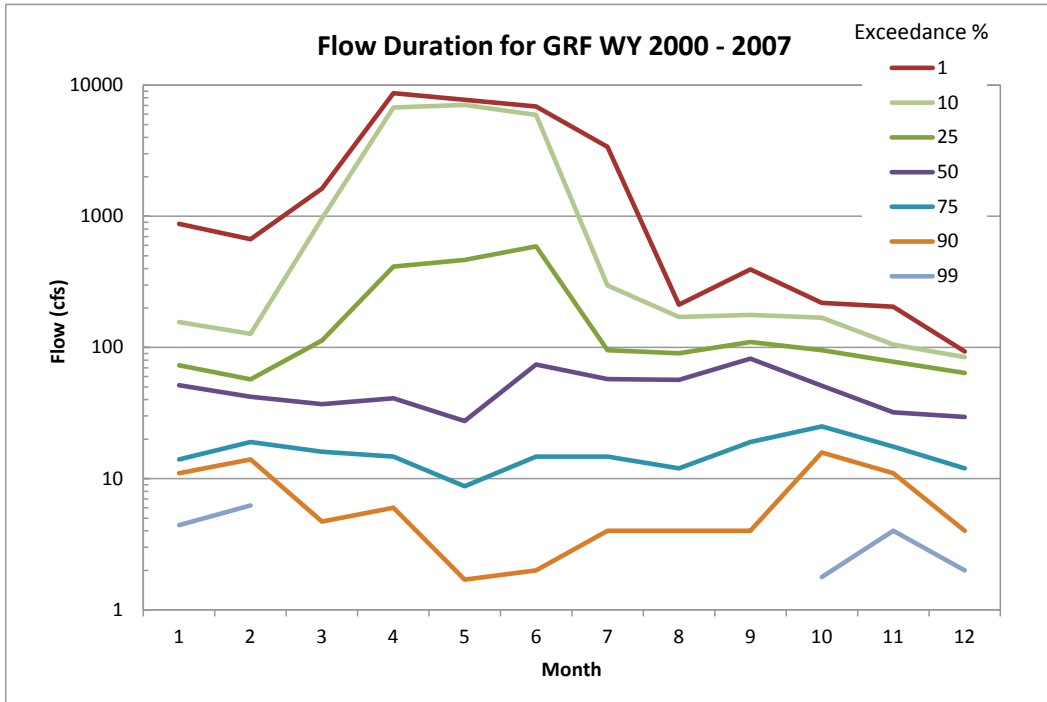


Figure C-2.—Monthly flow duration at GRF located in Reach 2A for WY 2000 through 2007.

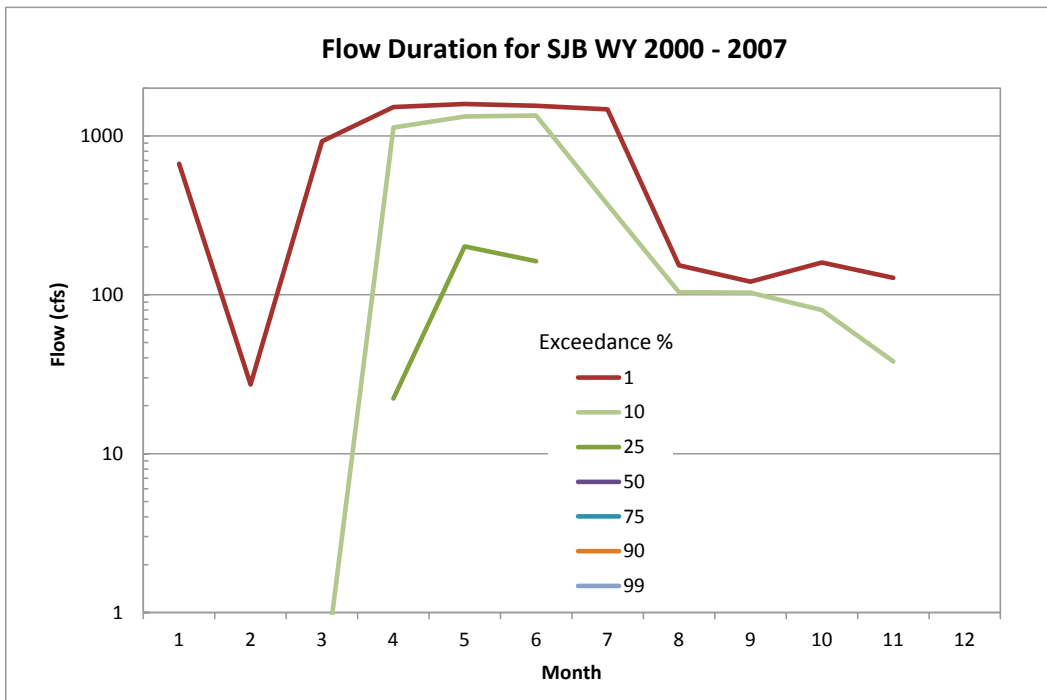


Figure C-3.—Monthly flow duration at SJB in Reach 2B for WY 2000 through 2007.

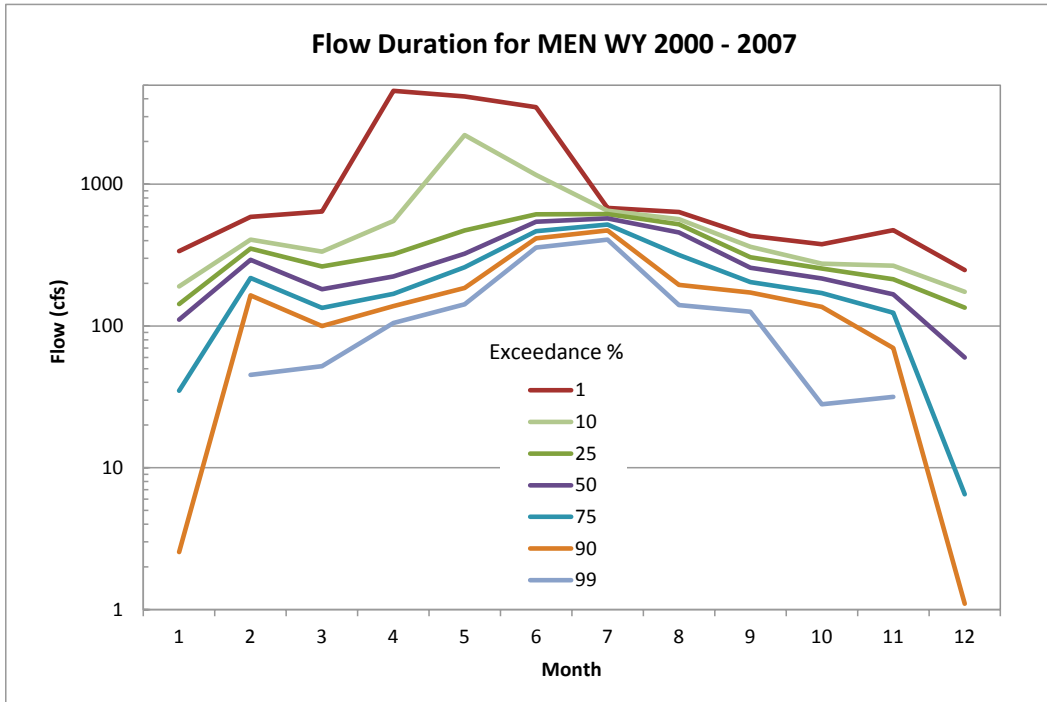


Figure C-4.—Monthly flow duration at MEN in Reach 3 for WY 2000 through 2007.

C.1.2 Simulated Flows under SJRRP

The future hydrology in Reach 2B will be substantially different than historical hydrology because of the SJRRP. The restoration flow schedules for Reaches 2 and 3 as defined by the Settlement are given in figure C-5 and figure C-6, respectively. However, the actual flows in the reach will also be influenced by flood operations, which can increase or decrease flows in a given year. Hydrologic simulation is necessary to develop a full range of hydrologic scenarios which will be used to analyze the performance of the floodplain design. A RiverWare hydrologic model was developed by TSC [Reclamation, 2012b]. The RiverWare model uses historical tributary and inflow data and operates the San Joaquin system consistent with the Restoration.

RiverWare simulated flows under SJRRP for the period using the historical inflows from 1923 - 2003 is shown in figure C-7 (GRF), figure C-8 (SJB), figure C-9 (MEN), and figure C-10 (JBP). The highest flows are limited to 4,500 cfs in Reach 2B. The flow is zero more than 10 percent of the time in Reach 2B in the month of May. This is because there is a forecast component in the RiverWare model when a more conservative flow forecast is used to choose the year type for the month of May. Whereas after May, a more accurate forecast is available and more flow will generally be available for restoration flows.

It is likely that when flood releases are occurring in the James Bypass, flows will be limited in Reach 2B because the capacity of Reach 3 and 4A is 4,500 cfs.

Therefore, more flow from the SJR will have to be released into the Chowchilla Bypass. An example of that occurred in WY 2011 during the flood release in April. The flow in Reach 2A was over 4,000 cfs, but the flow in Reach 2B was decreased to less than 500 cfs because of flows entering the SJR from James Bypass (figure C-11). Another example of the potential flood operations in Reach 2B is given in figure C-12 based upon simulated flows for WY 1986 under Restoration operations. The flows in Reach 2B under flood operations were decreased to less than 1,500 cfs because flows from James Bypass were near 4,000 cfs.

To provide information for floodplain inundation analyses, the daily average flow that is exceeded for various periods of time is also computed in table C-2.

The simulated hydrograph at the upstream end of Reach 2A for the period WY 1953 through 2002 is given in figure C-13. This 50-yr-period is used in the sediment transport analysis. Additional hydrologic scenarios will be used to define the potential channel response once the preferred option is selected. The specific hydrologic scenario is not expected to affect relative channel response between options.

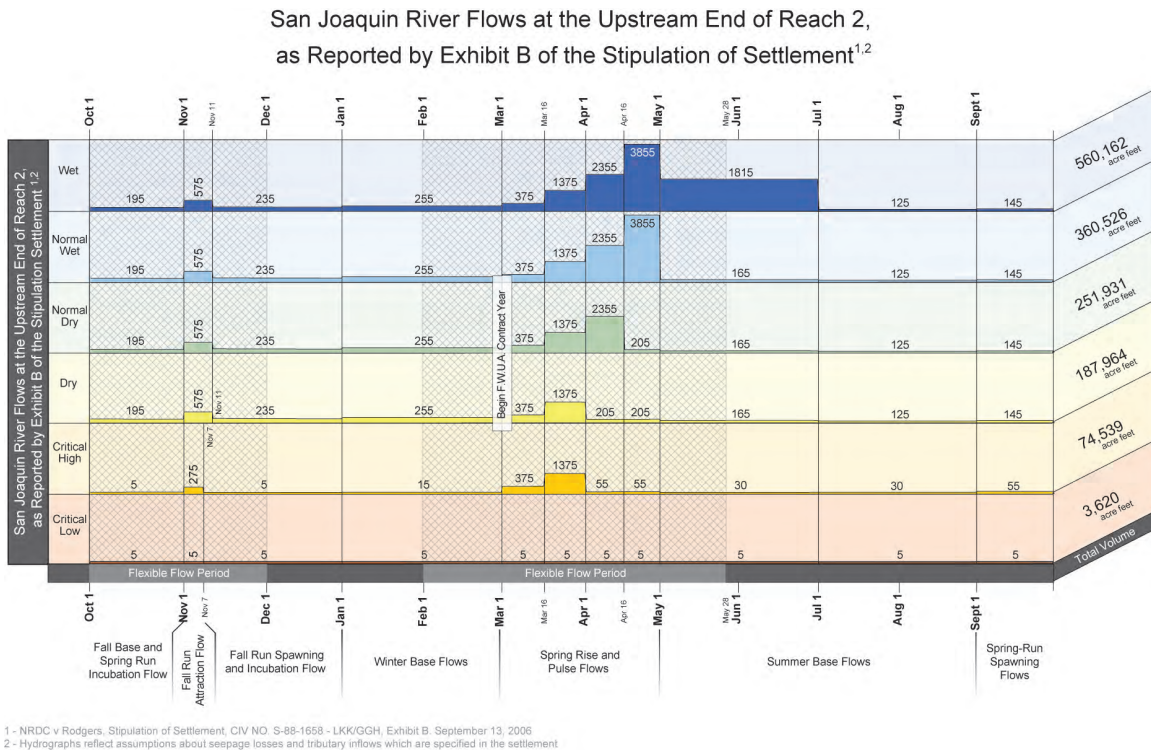
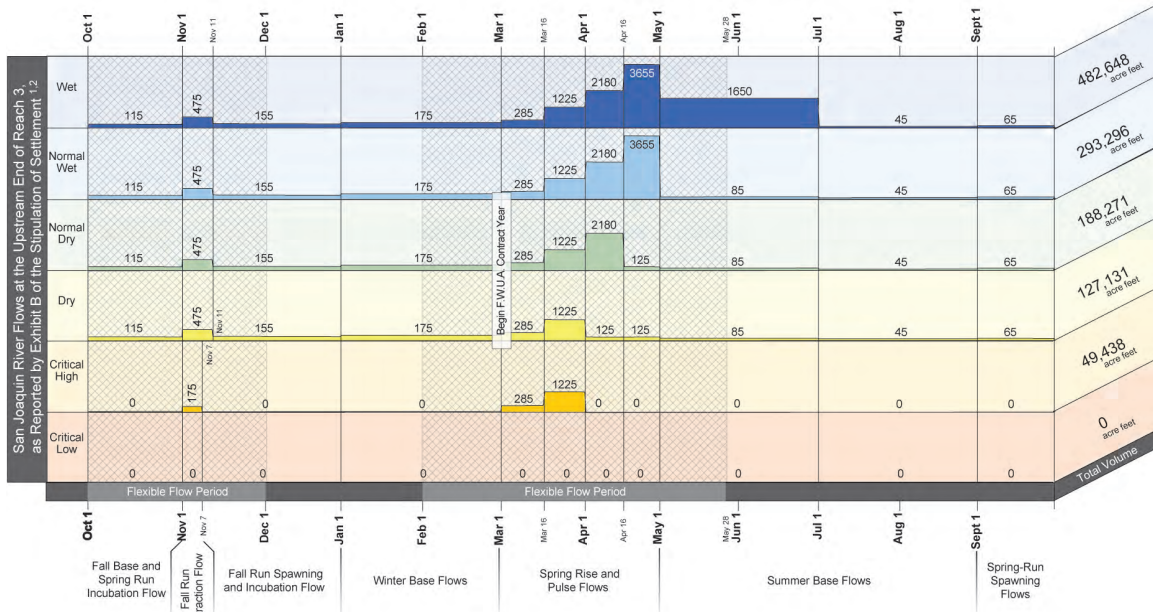


Figure C-5.—San Joaquin River flows at upstream end of Reach 2 as reported in Exhibit B of the Stipulation of Settlement.

San Joaquin River Flows at the Upstream End of Reach 3,
 as Reported by Exhibit B of the Stipulation of Settlement^{1,2}



1 - NRDC v Rodgers, Stipulation of Settlement, CIV NO. S-88-1658 - LKK/GGH, Exhibit B, September 13, 2006
 2 - Hydrographs reflect assumptions about seepage losses and tributary inflows which are specified in the settlement

Figure C-6.—San Joaquin River flows at upstream end of Reach 3 as reported in Exhibit B of the Stipulation of Settlement.

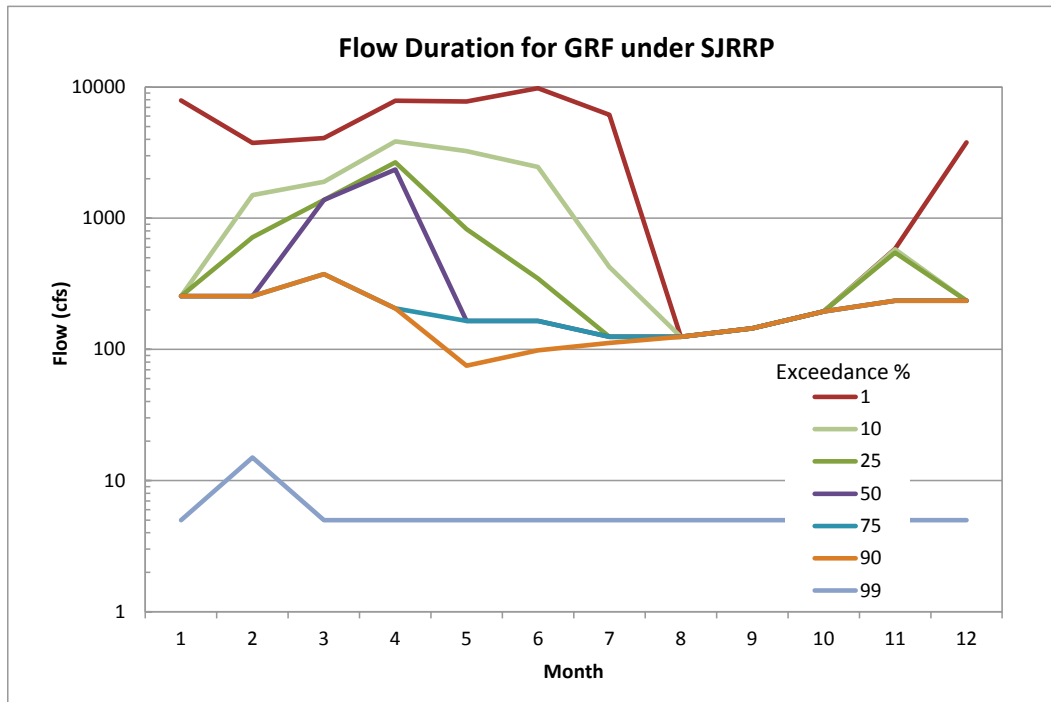


Figure C-7.—Simulated monthly flow duration at GRF in Reach 2A under the SJRRP.

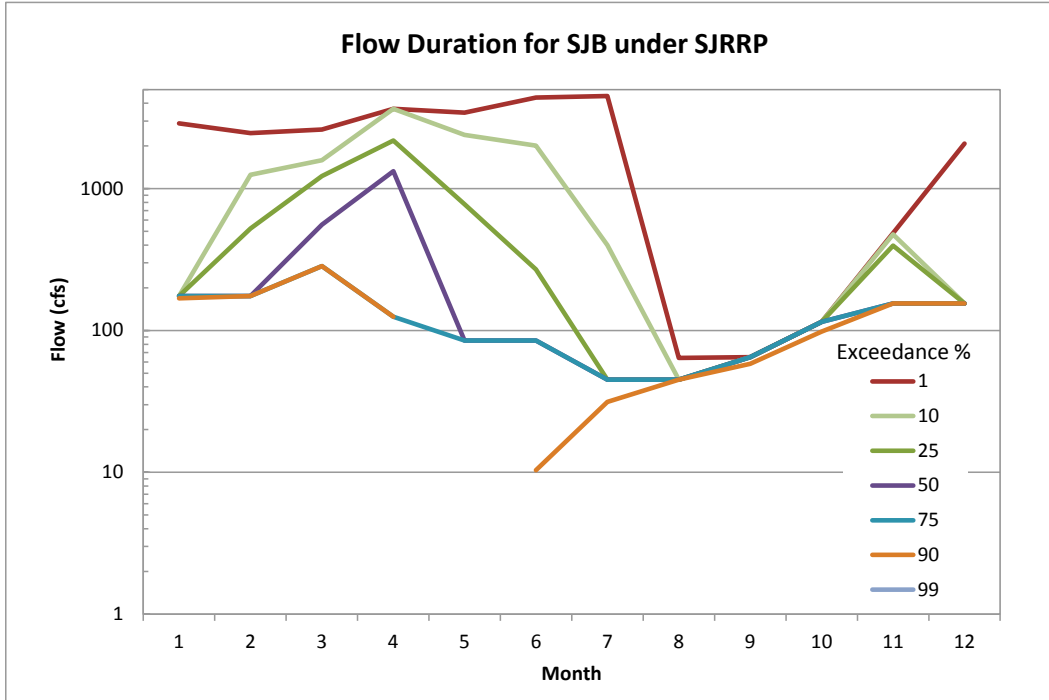


Figure C-8.—Simulated monthly flow duration at SJB under the SJRRP.

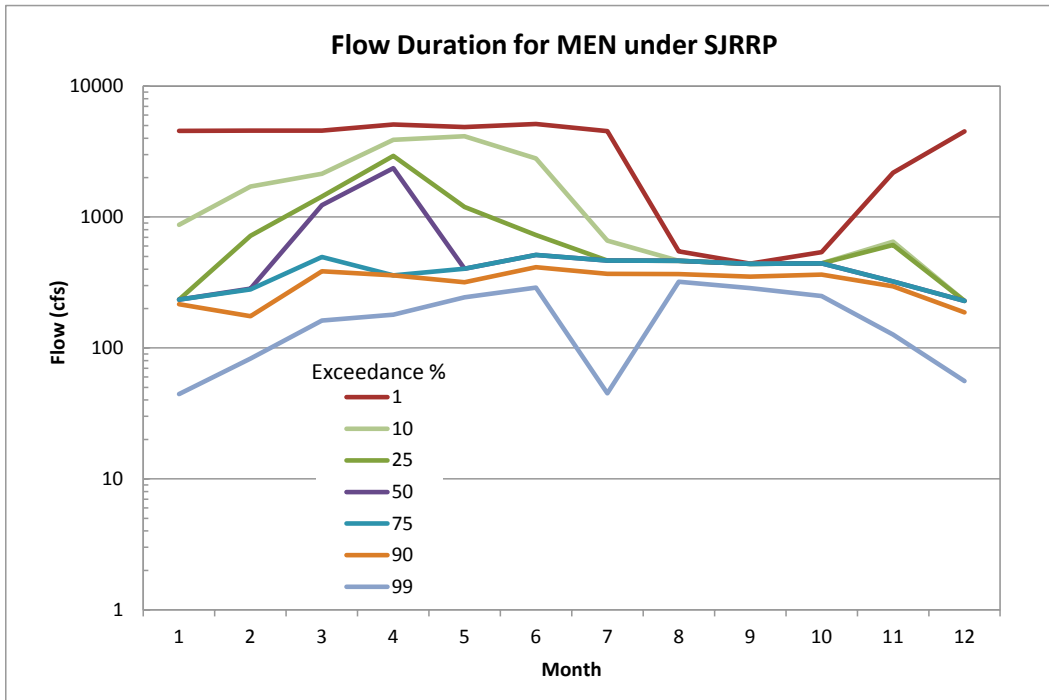


Figure C-9.—Simulated monthly flow duration at MEN in Reach 3 under the SJRRP.

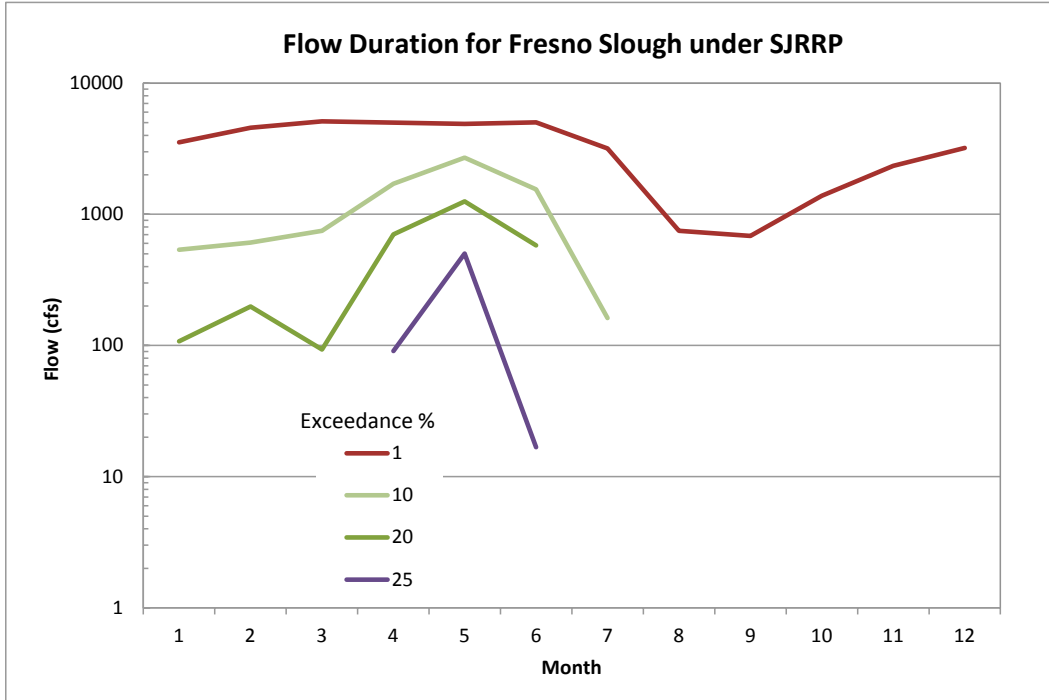


Figure C-10.—Simulated monthly flow duration at JBP under the SJRRP.

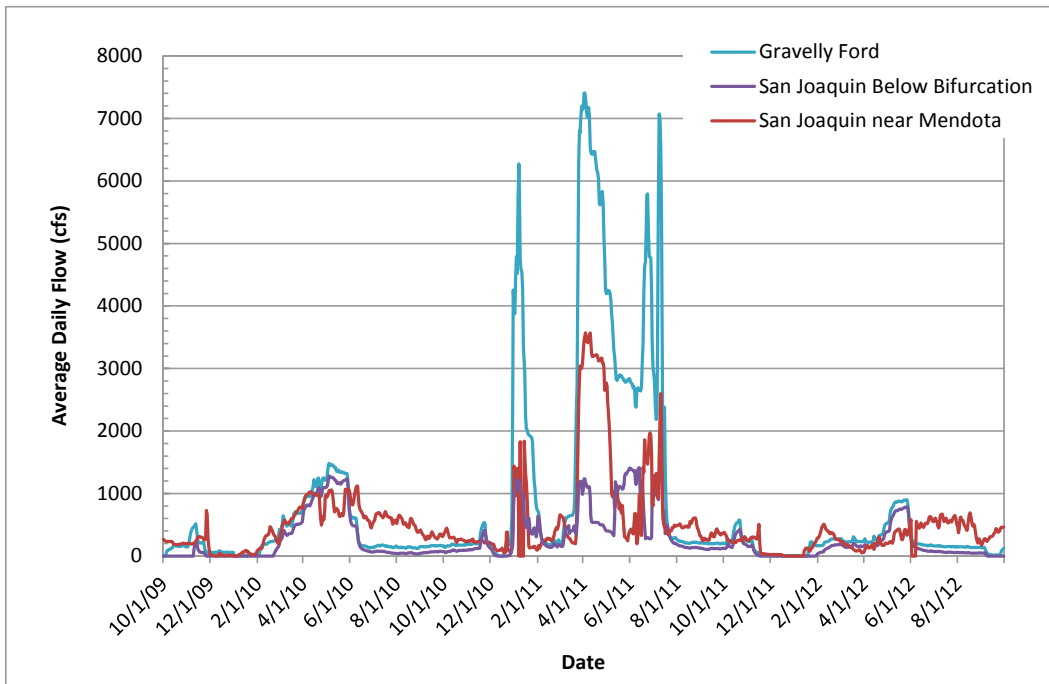


Figure C-11.—Measured daily average flows at GRF, SJB, and MEN for WY 2010 through 2012.

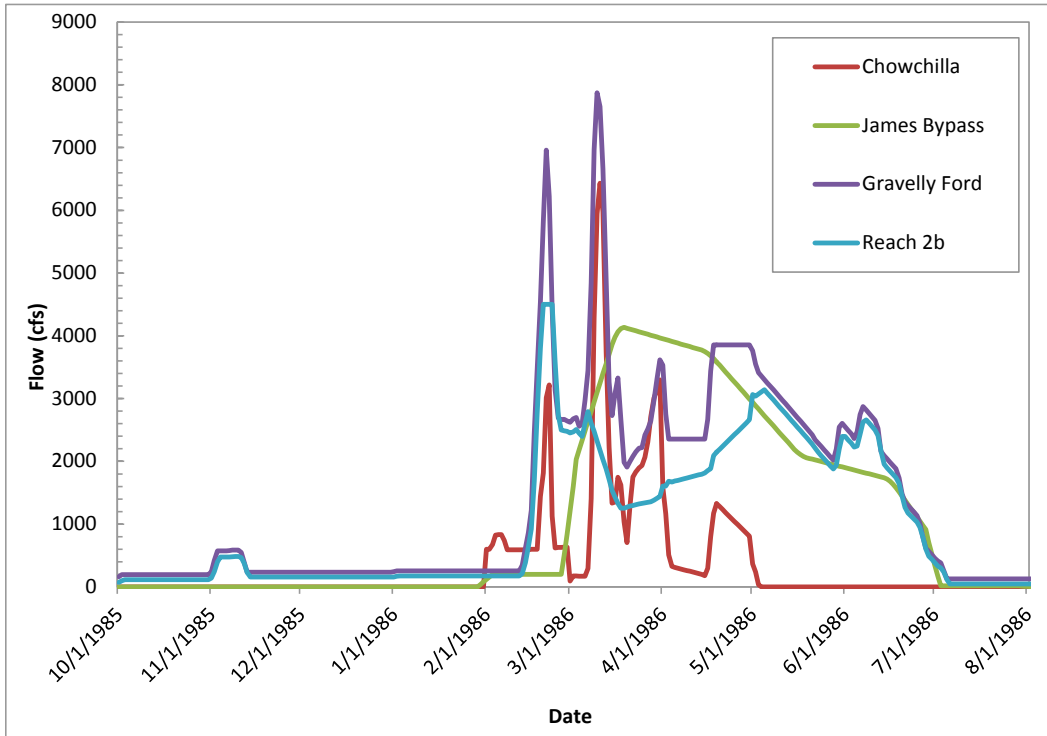


Figure C-12.—Simulated flows for WY 1986 under restoration operations.

Table C-2.—Return Period of Flow above a Given Level Based Upon Simulated Daily Average Flows from River Ware

| Return Period | Flow (cfs) That Is Exceeded for a Given Number of Days | | | | |
|---------------|--|-------|-------|-------|-------|
| | 1 | 2 | 7 | 14 | 21 |
| 50 | 4,531 | 4,507 | 4,500 | 4,445 | 4,061 |
| 20 | 4,500 | 4,500 | 4,309 | 3,655 | 3,655 |
| 10 | 4,049 | 3,835 | 3,655 | 3,473 | 3,144 |
| 5 | 3,655 | 3,655 | 3,655 | 2,889 | 2,236 |
| 3 | 3,655 | 3,655 | 3,629 | 2,338 | 2,180 |
| 2.33 | 3,655 | 3,655 | 2,863 | 2,180 | 2,180 |
| 2 | 3,117 | 2,870 | 2,180 | 2,180 | 1,917 |
| 1.5 | 2,180 | 2,180 | 2,180 | 1,739 | 1,225 |
| 1.11 | 1,225 | 1,225 | 1,225 | 1,207 | 519 |

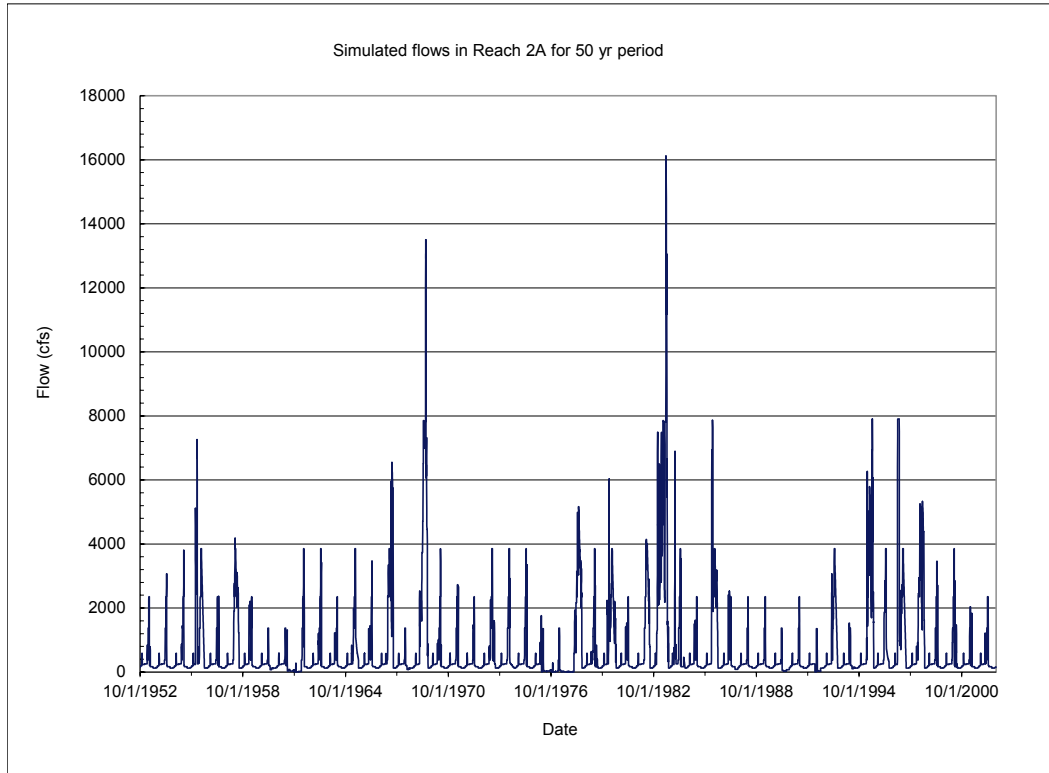


Figure C-13.—Flows simulated by RiverWare at upstream end of Reach 2A for WY 1953 through 2002.

C.2 Sediment Transport and Geomorphic Context

C.2.1 Historical Aerial Photography

Historical aerial photography is useful to determine conditions prior to the construction of Friant Dam and the flood bypass system. Recent aerial photography will also aid in the development of current designs. Aerial photography for years 1937, 1998, 2007, and April 27, 2011 is given in Appendix B. There are also 1914 California Debris Commission maps that cover the area.

The earliest aerial photographs were in 1937 during a time the reach was already extensively impacted by agriculture and the presence of Mendota Dam (built in 1871). The reach still had a much more extensive riparian corridor in 1937 than today, especially on the inner bends of the river. The main channel was much wider and the exposed sand bars were extensive. The flows were considerably higher in Reach 2B prior to the construction of Friant Dam, completed in 1942 [Reclamation, 2009a].

Table C-3.—Historical Aerial Photography Used in the Floodplain Design

| Date | Photography Type | Estimated Flow in Reach 2B (cfs) |
|----------------|------------------|-----------------------------------|
| 1914 | CDC maps | unknown |
| Oct 8, 1937 | Black and White | 1,120 cfs from USGS gage 11251000 |
| 1998 | Black and White | unknown |
| 2007 | Color | 0 cfs |
| April 27, 2011 | Color | 453 cfs from USGS gage 11253130 |
| June 2, 2011 | Infrared | 1,350 cfs from USGS gage 11253130 |
| July 20, 2011 | Infrared | 442 cfs from USGS gage 11253130 |

C.2.2 Measured Sediment Loads

Reclamation [2014] summarizes the sediment loads measured by U.S. Geological Survey (USGS) in the project reaches of the SJRRP that occurred in WY 2010 through 2012. The sediment information collected at these sites is given in table C-4 and the measurement locations are given in figure C-1.

At the measurement location within Reach 2B, SJB, the measured suspended sediment concentrations as a function of flow rate are given in figure C-14 and the measured bed load rates are given in figure C-15. The SJB measuring site is located just downstream of the Chowchilla Bifurcation Structure in Reach 2B. The measured velocities are low with a maximum measured velocity of approximately 1.75 ft/s; however, the maximum measured flow was only 1,320 cfs. The bed material at the gage is dominated by medium sand in the range of 0.25 to 1 mm, with approximately 9 percent of the bed material less than 0.25 mm.

Table C-4.—Information Collected at Sampling Sites for WY 2010 to 2012

| Sediment Sample Site | WY 2010 | | | WY 2011 | | | WY 2012 | | |
|----------------------|----------|----------------|--------------|----------|----------------|--------------|----------|----------------|--------------|
| | Bed Load | Suspended Load | Bed Material | Bed Load | Suspended Load | Bed Material | Bed Load | Suspended Load | Bed Material |
| Ledger | | | | X | | | | | |
| H41 | X | X | | X | X | X | X | X | X |
| SKB | X | X | | X | X | X | X | X | X |
| GRF | X | X | | X | X | X | X | X | X |
| Lower 2A | | | | X | X | | X | X | |
| SJB | X | X | | X | X | X | X | X | X |
| MEN | X | X | | X | X | X | X | X | X |

C.2.2.1 Bed Load

Because of the low flows and velocities, the maximum measured bed load discharge at SJB was only 33 tons/d, whereas the maximum measured bed load at GRF was over 4,000 tons/d. The bed load is not well correlated with flow rate and while the largest measured bed load rates occurred during the highest flows, some of the lowest measured bed load rates have also occurred during the highest flows. Most likely due to the fact that the Chowchilla Bifurcation is located immediately upstream and the flow in the SJR upstream of the structure can be as high as 8,000 cfs while the flow in the river below the structure is less than 1,500 cfs. Therefore, the sediment transport just downstream of the structure may be more a function of the conditions upstream of the structure than the flow at the gage site. It should be noted, however, that the same variation exists in measured bed load and suspended load at flows below 2,000 cfs at GRF. At low transport rates, the relative sampling variability can be high. At flow rates less than 1,500 cfs, the measured bed load at SJB is similar to the measured bed load at GRF with variation between 1 ton/d to 30 tons/d.

C.2.2.2 Suspended Load

The suspended sediment concentrations were similar in magnitude to those measured at GRF, with maximum total suspended concentrations of less than 30 mg/l sampled at SJB (figure C-14). The maximum suspended sand concentration was 9 mg/l, with typical concentrations between 1 to 4 mg/l.

The diameter for which all material, coarser than will be transported as bed load, was less than 0.35 mm for all flows measured. It is expected that the majority of the bed material is transported as bed load at SJB.

C.2.3 Estimated Sediment Budget

The annual sand loads estimated in Reclamation [2014] are given in figure C-18. The sediment budget for WY2011 is summarized below.

C.2.3.1 SKB to GRF (RM 232.1 to 227.6)

There is a large gravel pit complex at RM 233 that may trap significant amounts of sand in transport at gage SKB. However, the flow paths at high flows are complex and some flow paths that bypass the gravel pits may transport sand around the pits.

The best estimate of sand transport at GRF was 90,000 tons, which resulted in a net sand export of approximately 76,000 tons from this reach in WY 2011. Even though this reach was one of the shortest, it had the highest net sand deficit of any of the reaches. It is likely that this reach has large amounts of sand available for transport whereas the reaches upstream of it do not.

There are several potential sites where bank erosion and/or erosion of floodplain surfaces is possible, but no explicit measurement of these processes has been performed in this reach. There is also the potential for significant vertical bed erosion in the reach from SKB to GRF because there are no significant bedrock controls.

Because the high flow sand load measurements occurred approximately 4,000 ft downstream of the GRF gage site, this reach actually extends from SKB to 4,000 ft downstream of the GRF gage site.

C.2.3.2 GRF to Lower Reach 2A (RM 227.6 to 219.3)

The sand transport in WY 2011 at the lower Reach 2A site was estimated from bed load measurements at flows below 1,000 cfs in WY 2012. Therefore, there is a large uncertainty in the annual sediment load values at the gage in lower Reach 2A for WY 2011 because the flows at this site exceeded 7,000 cfs. According to the best estimates, there is a net export of 50,000 tons of sand in the reach.

There are several bank erosion sites within Reach 2A, but no explicit accounting of the bank erosion volume has been performed. The low flow channel is not well defined throughout most of the reach because until 2009 this reach did not receive base flows and was lacking significant riparian vegetation. Therefore, it is difficult to determine bank lines and differentiate between the channel bed and floodplain.

C.2.3.3 Lower 2A to SJB (RM 219.3 to 216.0)

The lower Reach 2A sampling site is located approximately 3.3 miles upstream of the SJB. In WY 2011 the maximum flow in Reach 2B was limited to 1,415 cfs, and the majority of flow was routed into the SJB. The vast majority of the sediment also entered the SJB and was not routed into Reach 2B.

The high flows in WY 2011 were estimated to erode approximately 36,000 tons of total sediment from the 2.7 miles upstream of Chowchilla Bifurcation [Tetra Tech, 2012c], with the majority of that sediment in the sand size range.

Over the long term, however, this reach is expected to be relatively stable because of the grade control imposed by the Bifurcation structure and the limited ability of the reach to store sediment. The structure has been in place since the 1960's and bed elevations have likely stabilized to a dynamic equilibrium, meaning that there are likely fluctuations of bed elevations in any given year depending upon the inflow and gate operations, but that over many years there are no significant trends in aggradation or degradation.

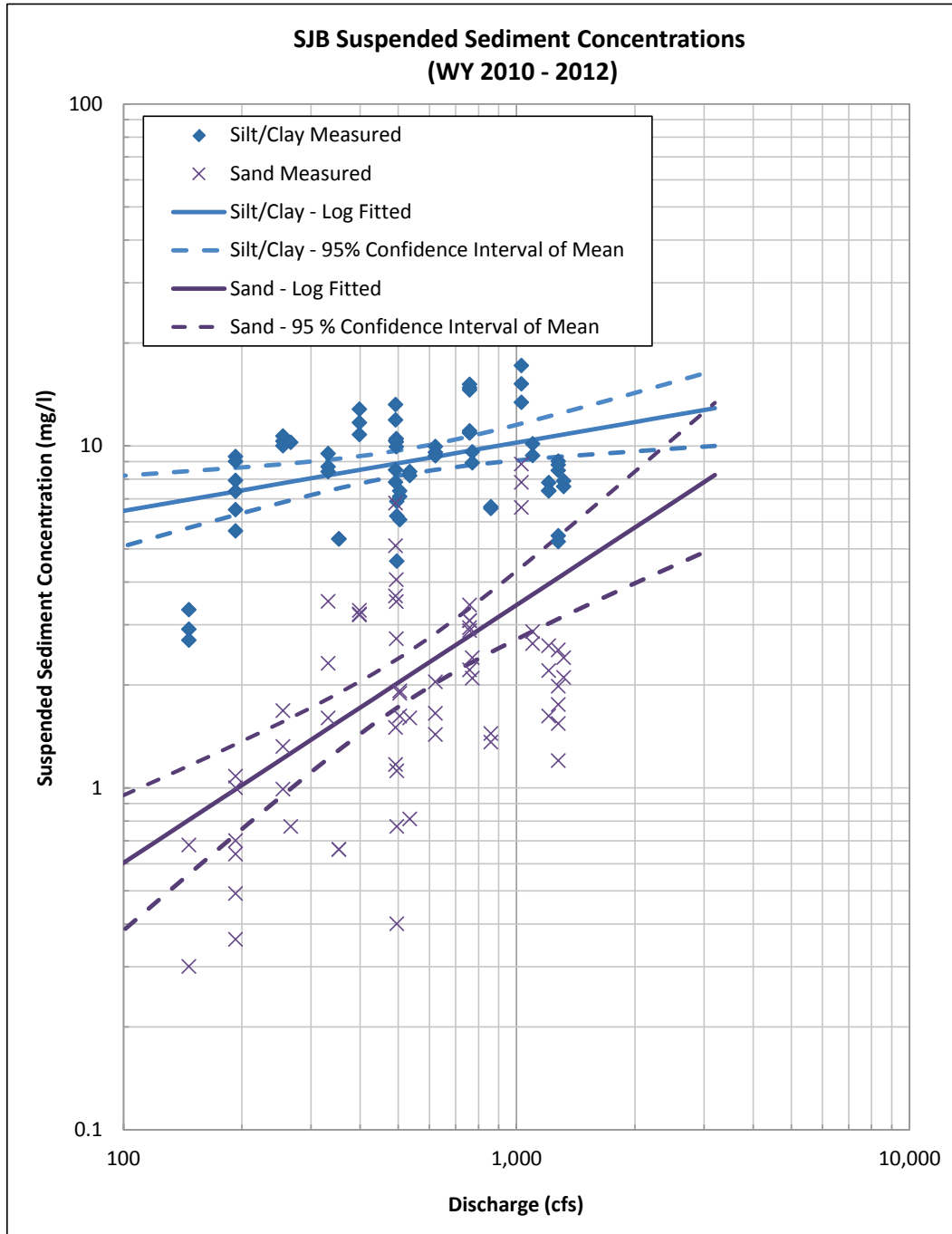


Figure C-14.—Measured suspended sediment concentration at SJB for WY 2010 through 2012.

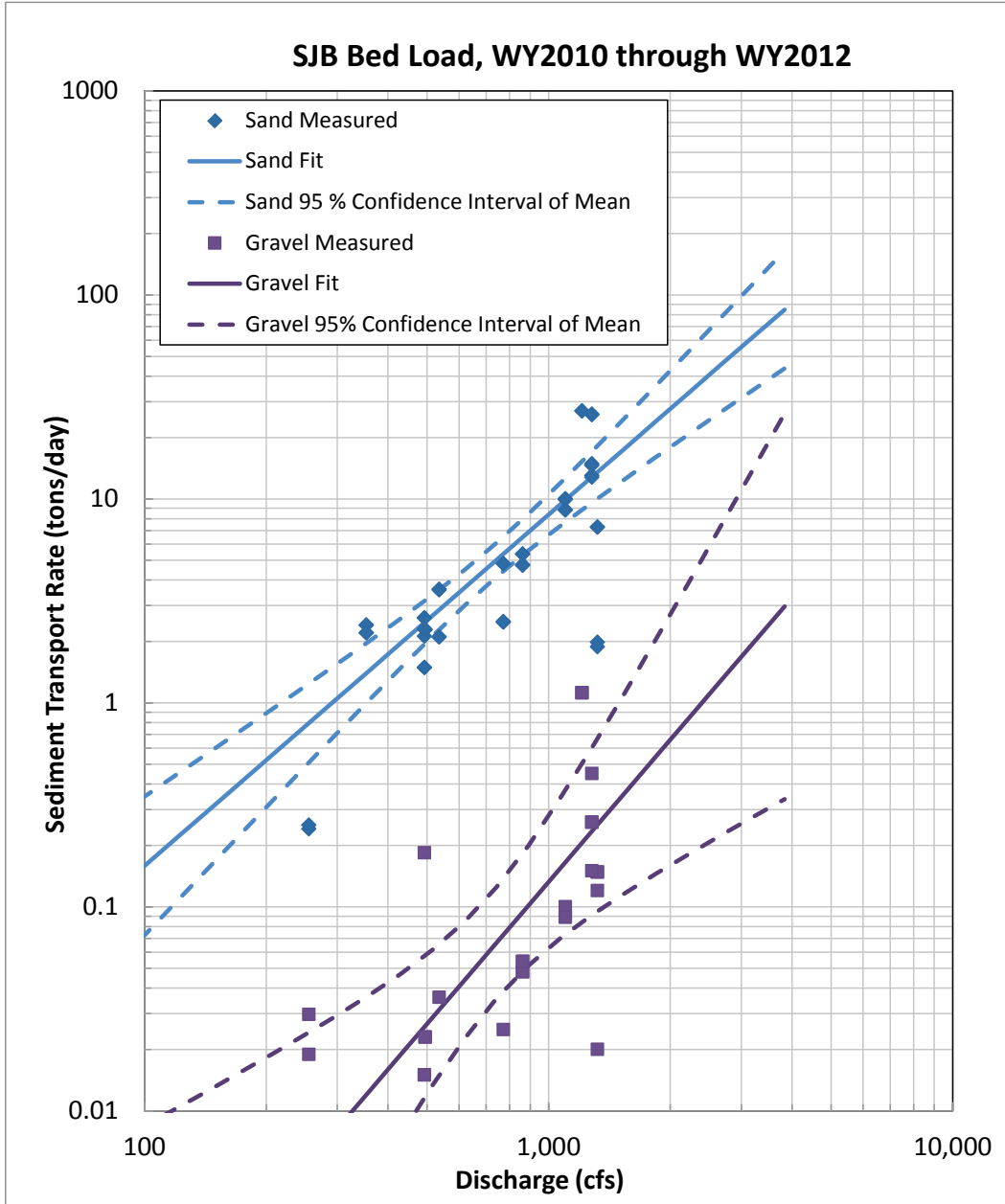


Figure C-15.—Measured gravel and sand bed load transport rate at SJB for WY 2010 - 2012.

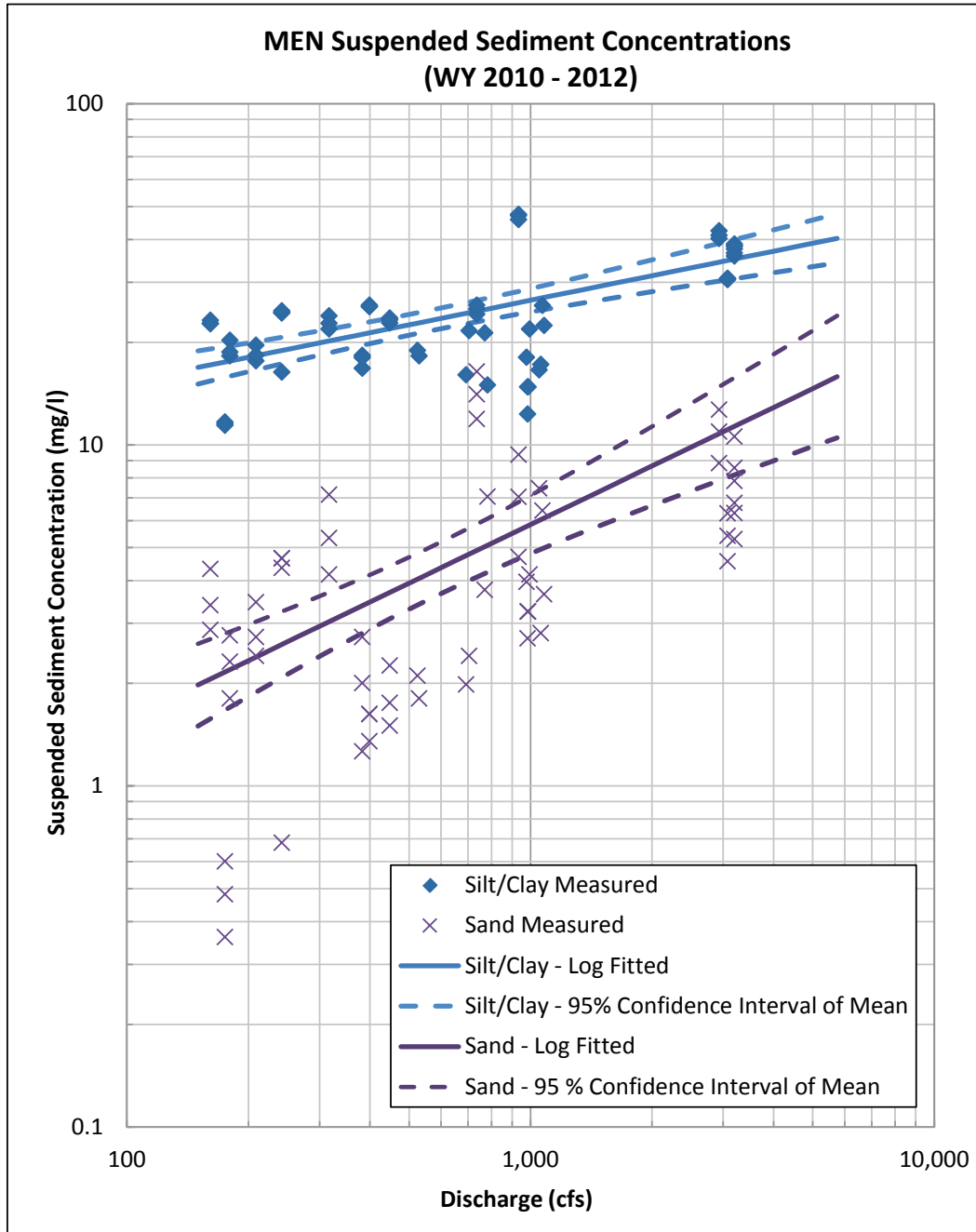


Figure C-16.—Measured suspended sediment concentration MEN for WY 2010 - 2012.

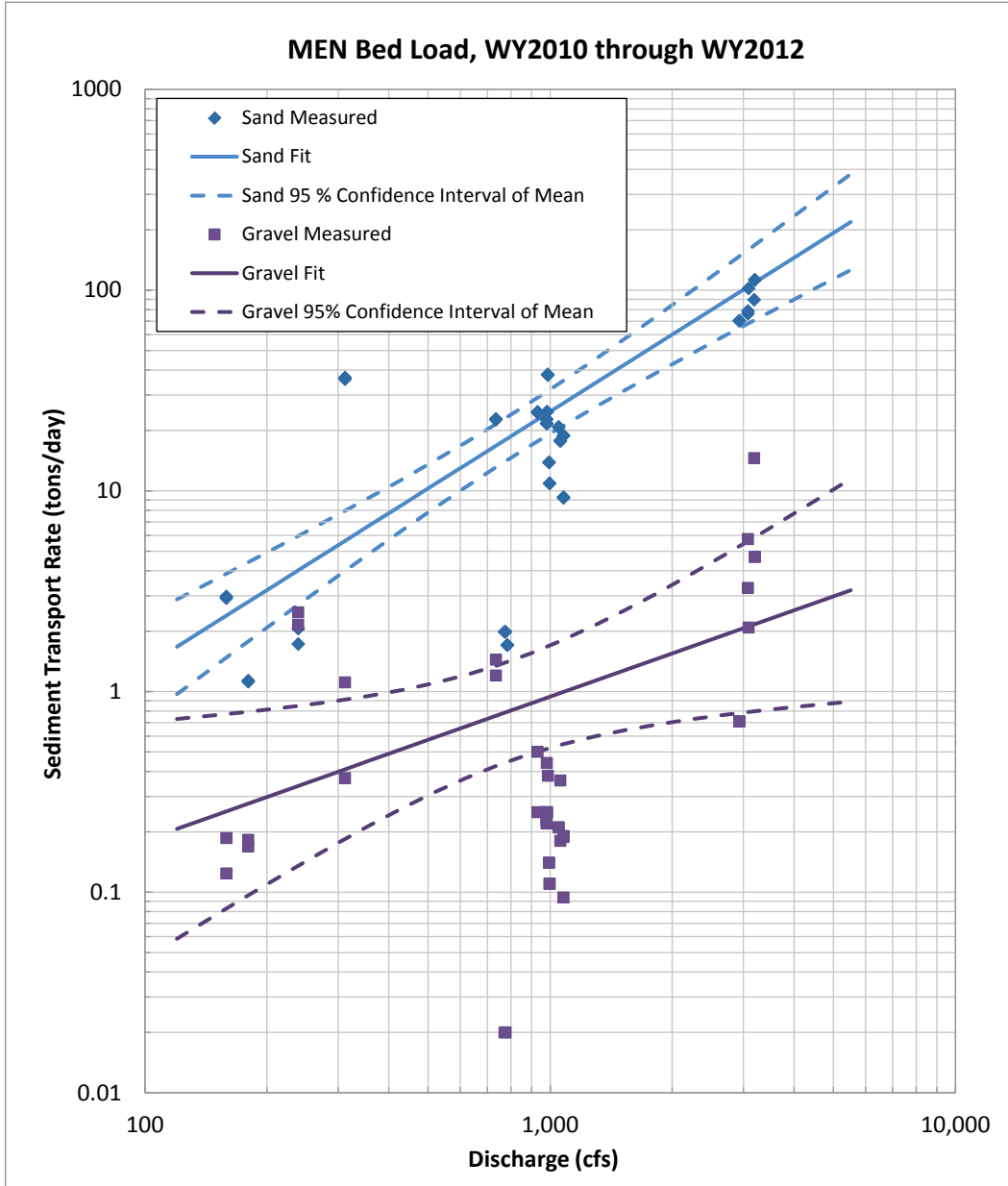


Figure C-17.— Measured bed load on San Joaquin at MEN for WY 2010 - 2012.

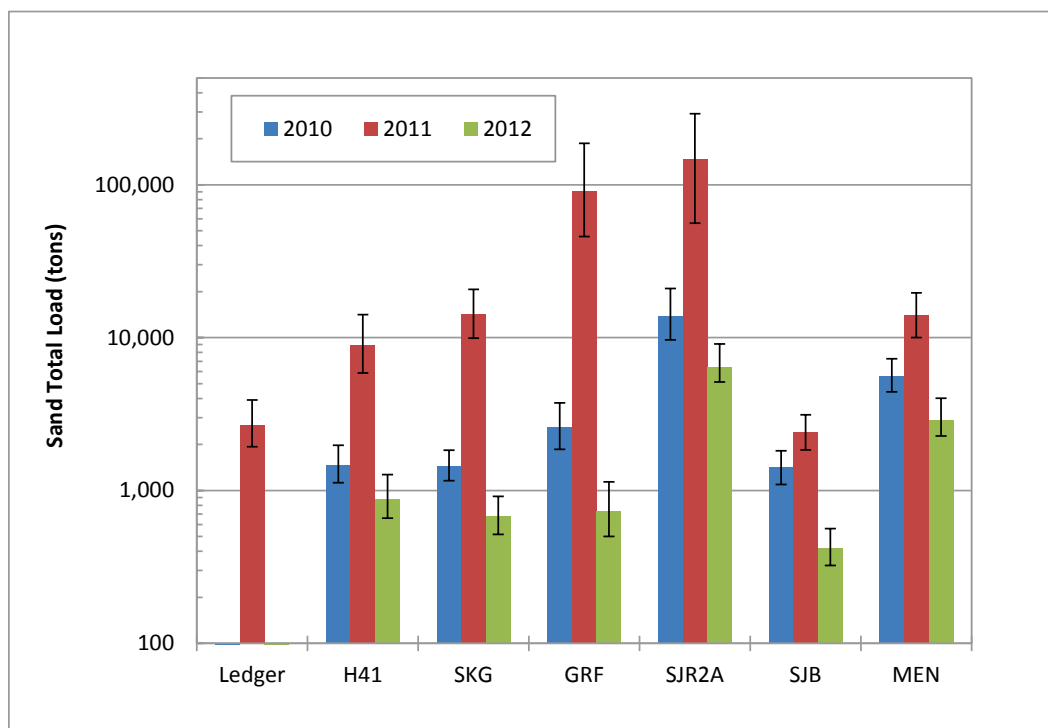


Figure C-18.—Estimated annual total sand sediment loads in WY 2010 - 2012 for sediment measurement locations.

C.2.3.4 SJB to MEN (RM 219.3 to 202.1)

Only 2,000 tons of sand transport were estimated at SJB during WY 2011 and 14,000 tons of sand transport at MEN. Potential sources of sand between SJB and MEN are the Fresno Slough and the bed and banks of Reaches 2B and 3, which include the sediment stored in Mendota Pool. Mendota Pool may still trap some sediment but the dam has been in place for over 90 years and its ability to trap additional sediment may be limited. Therefore, during high flow years when the flash boards are removed, the pool may act as a source of sand sized material.

No sediment supply study has been conducted on the Fresno Slough so it is difficult to determine if sand sized sediment is being transported through James Bypass and the Fresno Slough area.

Because the flow was limited to 1,400 cfs in Reach 2B, it is unlikely that any significant erosion occurred in this reach, but it is possible that some limited bed erosion in Reach 3 occurred. Sand contributions from Reach 2B and the Fresno Slough may, however, be sufficient to prevent significant erosion in Reach 3.

C.2.4 Bed Material

There have been several measurements of bed material at the sediment load measurement sites listed in table C-1 table C-5 from 2010 through 2012. There

were also bed material measurements in Reach 2A and Reach 3 by Reclamation in February of 2008 (Reclamation, 2008). A summary of the results is given in table C-5 and a plot of the sediment gradations for various river miles is given in figure C-19.

Table C-5.—Summary of Bed Material Measurements in Reach 2 and 3

| % Finer than (mm) | | | | | | | | | | | Location | Source |
|-------------------|-------|------|------|------|------|------|------|------|------|------|--|-------------|
| 0.0625 | 0.125 | 0.25 | 0.5 | 1 | 2 | 4 | 8 | 16 | 32 | 64 | | |
| 0.1 | 0.5 | 3.0 | 13.7 | 35.7 | 55.1 | 62.1 | 67.2 | 78.0 | 93.5 | 100. | at gage GRF | USGS |
| 1.0 | 1.4 | 3.4 | 18.5 | 51.1 | 75.7 | 84.1 | 87.6 | 94.6 | 100. | 100. | RM 226.8 ave of 3-5,3-6,3-7 | Reclamation |
| 1.0 | 2.4 | 7.7 | 25.3 | 63.5 | 79.0 | 81.6 | 83.8 | 93.3 | 99.5 | 100. | RM 224.1 ave of 3-14, 3-15 | Reclamation |
| 1.9 | 3.1 | 8.7 | 40.3 | 80.5 | 96.7 | 99.6 | 99.9 | 100. | 100. | 100. | RM 223.3, ave of 3-17,3-19,3-20,2-11,2-10 | Reclamation |
| 1.9 | 3.1 | 8.7 | 40.3 | 80.5 | 96.7 | 99.6 | 99.9 | 100. | 100. | 100. | RM 216.2 ave of 3-17,3-19,3-20,2-11,2-10 | Reclamation |
| 0.0 | 3.1 | 9.1 | 23.6 | 57.3 | 83.7 | 96.2 | 98.6 | 99.5 | 99.9 | 100. | at gage SJB | USGS |
| 0.8 | 2.3 | 9.1 | 36.6 | 69.6 | 91.2 | 98.0 | 99.9 | 100. | 100. | 100. | at gage MEN | USGS |

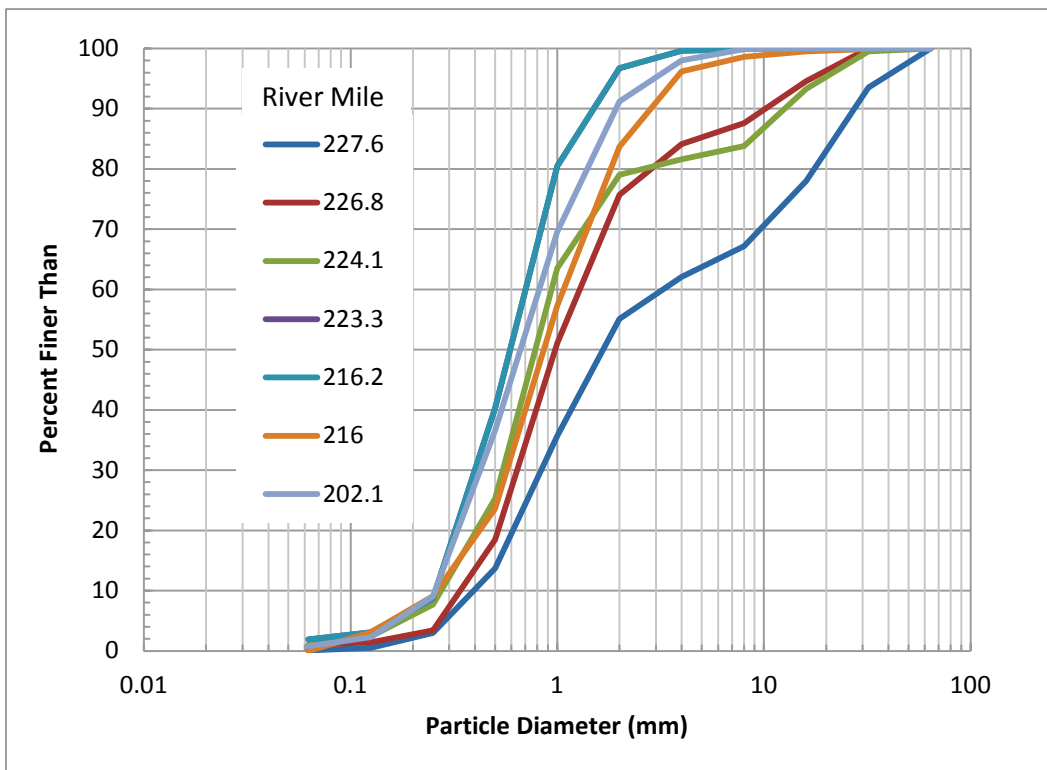


Figure C-19.—Average bed material gradations in SJR (by RM).

C.5 Hydraulic Modeling

The HEC-RAS model for Reach 2B under project conditions was described in Attachment D – Hydraulics Modeling Memo of the Project Description [SJRRP, 2012b]. The HEC-RAS model used for Reach 3 is documented in Tetra Tech [2013].

The HEC-RAS model for the Bypass was developed using Hydrologic Engineering Centers River Analysis System extension for use in ArcGIS (HEC-GeoRAS) 10.2 and appended to the downstream end of the Reach 2B model. HEC-GeoRAS 10.2 is an extension to ArcGIS 10.2 and available for download at: <http://www.hec.usace.army.mil/software/hec-georas/>. ArcGIS 10.2 is a GIS for working with maps and geographic information (<https://www.arcgis.com>). The channel excavation tools within HEC-RAS were used to create the initial excavated channel through the Bypass.

A more detailed 2D hydraulic analysis will be performed after more detailed structural design is performed. The detailed 2D analysis will aid in the fish passage assessment and in the design of the grade and bank stabilization features.

The cross section layout for the HEC-RAS model of Reaches 2B and 3 is shown in figure C-20.

C.6 Sediment Modeling

The Bypass, as well as the SJR upstream and downstream of the Bypass, is expected to evolve in time after the construction and operation of the Bypass. A mobile bed sediment transport model (SRH-1D) was used to evaluate the effect of the Bypass channel on the sediment transport and bed morphology from Reach 2B through Reach 3. The model used the HEC-RAS cross sections from Reach 2A through Reach 3 as documented in Tetra Tech [2013]. An equilibrium sediment load was assumed at the upstream end of Reach 2A, where the initial bed gradation and the sediment transport formula are used to compute the bed material load entering the simulated reach. Only bed material load is being simulated in this report and wash load is ignored. Because the model boundary is located approximately 10 miles upstream, there is little influence of the boundary condition on the results in Reach 2B.

The restoration flows as simulated using the RiverWare model described in section C.1.2—Simulated Flows under SJRRP were used in the simulation. A 50 year period using the historical flow input at Millerton Lake from WY 1953 to 2003, as if the SJRRP was in place, was used in the sediment transport simulations. The flows at the GRF, the upstream end of the model, are given in figure C-13. The bed material used in the simulation was taken from table C-5.

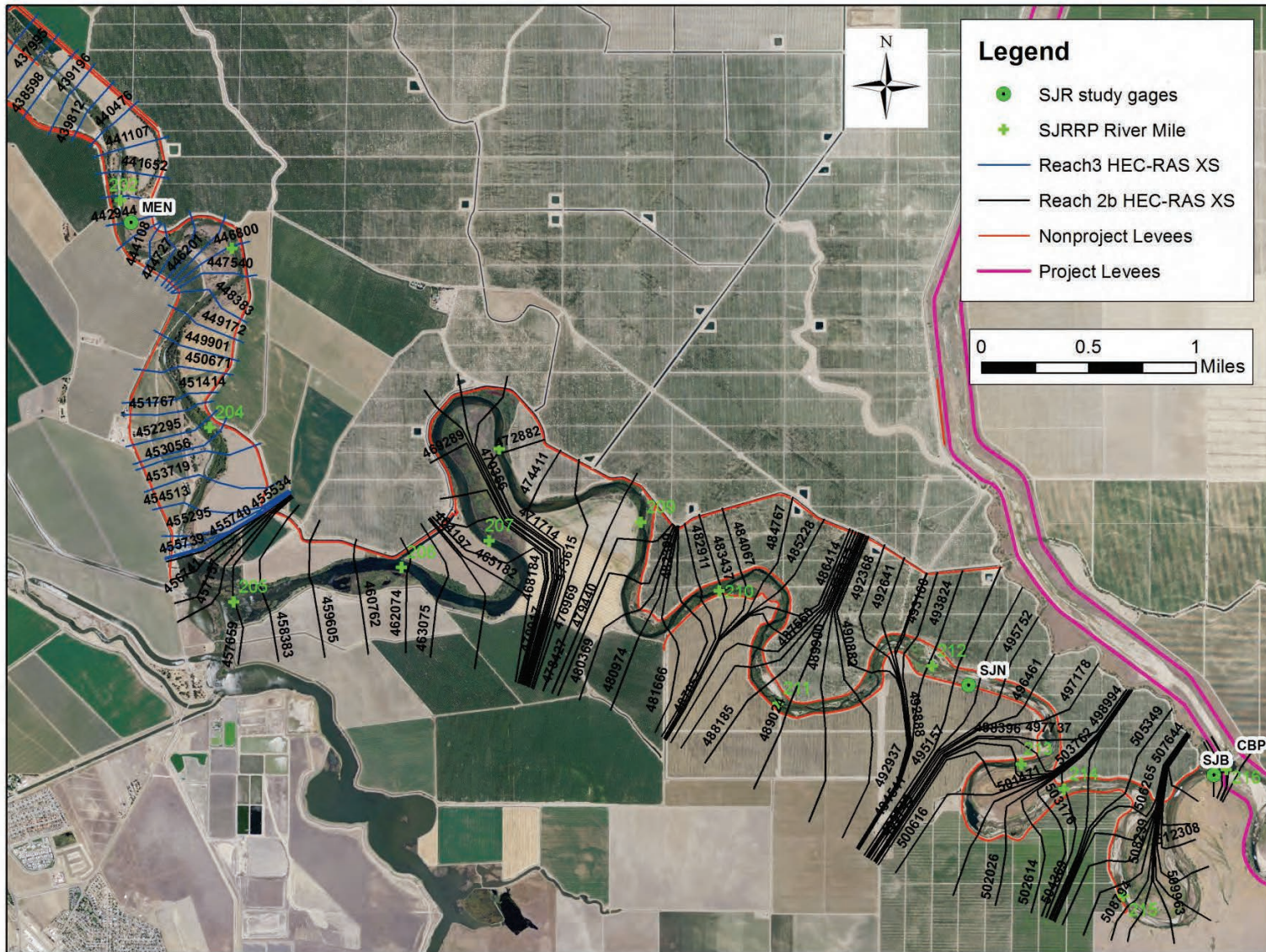


Figure C-20.—Cross section layout for Reaches 2B and 3. The Bypass cross sections are already shown in figure 4-1.

The extraction of flow and sediment at the Chowchilla Bifurcation is included into the sediment model. The flow routing is taken from the RiverWare simulation and the sediment extraction by the Bifurcation is assumed proportional to flow at the Bifurcation.

The addition of flow from Fresno Slough is also included in the model based upon the RiverWare simulations. No sediment is assumed to be contributed by Fresno Slough and this assumption is based upon the relatively large pool of slow moving water present where the James Bypass and Fresno Slough confluence, approximately 9 miles upstream of the Mendota Pool. The large pools are expected to trap most of the incoming sand sized sediment.

The rates of land subsidence were taken from table 2-3. The results with and without subsidence were evaluated.

C.6.1 Sediment Transport Capacity

To validate the choice of the sediment transport function used within the SRH-1D model, the measured sediment transport data at SJB and MEN were compared against the results from SRH-1D at the gage locations. The model only computed the sand and gravel load and the silt/clay fractions were ignored for the purposes of this simulation because the silt/clay fractions are not significantly represented in the channel bed. In Reach 2B and 3, the sand load is about two orders of magnitude greater than the gravel load [Reclamation, 2014]. Five different sediment transport functions were used within SRH-1D: Engelund and Hansen's Method [1972], Laursen's Formula [1958] and Modified Version [Madden, 1993], Wu et al. [2000], and Parker's Method [1990]. Each method is described below.

C.6.2 Engelund and Hansen's Method [1972]

Engelund and Hansen [1972] proposed the following transport function for use in primarily sand bed rivers:

$$f' \phi = 0.1 \theta^{5/2} \quad (\text{Eq. 9-1})$$

where:

$$f' = \frac{\tau}{\frac{1}{2} \rho V^2} \quad (\text{Eq. 9-2})$$

$$\phi = q_t / \sqrt{(s-1)gd^3} \quad (\text{Eq. 9-3})$$

$$\theta = \frac{\tau}{(\gamma_s - \gamma)d} \quad (\text{Eq. 9-4})$$

where f' = friction coefficient, g = gravitational acceleration; V = average flow velocity; q_t = total sediment discharge by volume per unit width; s = specific gravity of sediment; γ_s and γ = specific weights of sediment and water, respectively; d = median particle diameter; and τ = total shear stress along the bed.

C.6.3 Laursen's Formula [1958] and Modified Version [Madden, 1993]

Laursen's formula [1958] has both bed load and suspended load components and in theory could apply to both sand and gravel. It was expressed in dimensionally homogeneous forms by the American Society of Civil Engineers (ASCE) Task Committee [1971] as,

$$C_i = 0.01\gamma \sum_i p_i \left(\frac{d_i}{D} \right)^{7/6} (\phi_i - 1) f \left(\frac{U^*}{w_{fi}} \right) \quad (\text{Eq. 9-5})$$

where C_i = sediment concentration by weight per unit volume; $U^* = \sqrt{gDS}$; p_i = percentage of materials available in size fraction i ; w_{fi} = fall velocity of particles of mean size d_i in water; and D = average water depth. The parameter ϕ_i is a measure of the shear stress relative to the reference shear stress:

$$\phi_i = \theta_i / (\xi_i \theta_c) \quad (\text{Eq. 9-6})$$

where θ_c is the reference Shield's number; and θ_i = Shield's parameter of the sediment size class i computed as:

$$\theta_i = \tau_g / (\gamma(s-1)d_i) \quad (\text{Eq. 9-7})$$

where τ_g is the grain shear stress. The parameter ξ_i is the exposure factor, which accounts for the reduction in the critical shear stress for relatively large particles and the increase in the critical shear stress for relatively small particles:

$$\xi_i = (d_i / d_{50})^{-\alpha} \quad (\text{Eq. 9-8})$$

where α = a constant. Laursen assumed that $\theta_c = 0.039$ and that $\alpha = 0$, meaning that there is no hiding and exposure. SRH-1D adds the ability to compute the effect of mixtures by allowing the user to specify different values of θ_c and α .

Laursen's grain shear, τ_g , was computed as,

$$\tau_g = \frac{\rho V^2}{58} \left(\frac{d_{50}}{D} \right)^{1/3} \quad (\text{Eq. 9-9})$$

In the above equations, ϕ_i is important in determining bed load, and the parameter U^* / w_{fi} relates to suspended load. The functional relation $f(U^* / w_{fi})$ is given by Laursen (1958) in a graphical form and SRH-1D uses the following functions to approximate the curve:

$$\ln[f(\eta)] = 2.25 + 0.25\lambda + 6.9[1 - \exp(-0.085\eta)] - 0.37 \exp[-(\lambda - 3.8)^2] \quad (\text{Eq. 9-10})$$

where $\eta = U^* / w_{fi}$ and $\lambda = \ln(\eta)$.

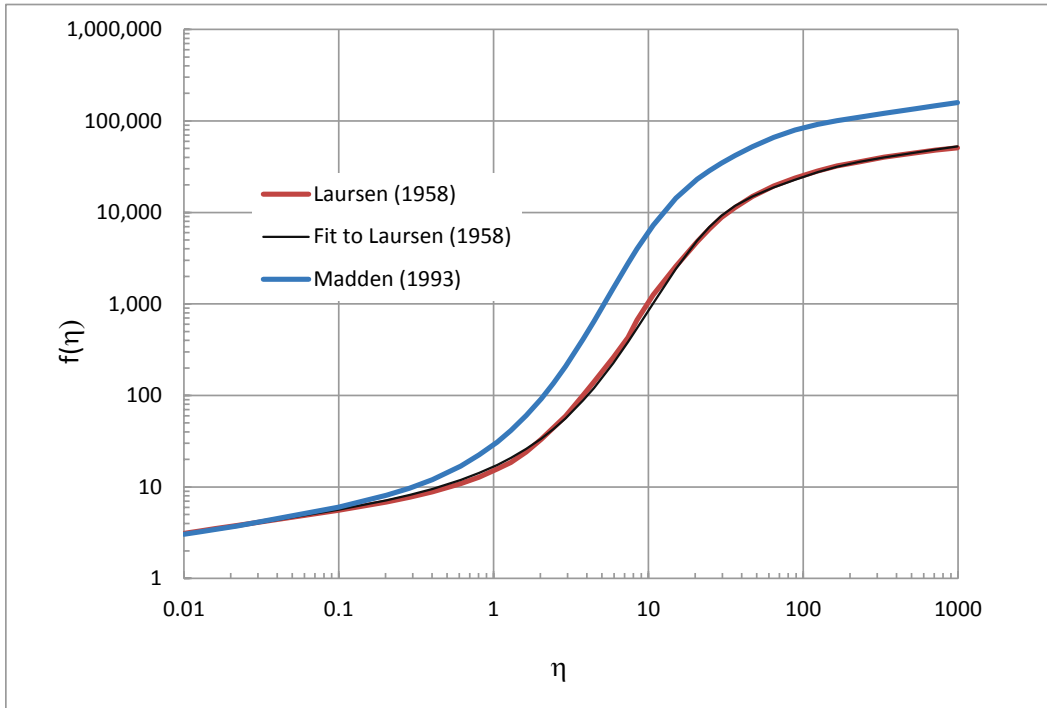


Figure C-21.—Comparison between Laursen’s [1958] function and fitted function.

Madden [1993] revised the Laursen relation to fit the sediment load discharge rating curves in the lower Arkansas River. The result was a curve similar in shape to Laursen, but one that predicts significantly higher transport rates as η increases. Both the original Laursen equation and the revised equation by Madden [1993] are implemented in SRH-1D. The fit equation for the Madden [1993] equation is:

$$\ln[f(\eta)] = 2.25 + 0.25\lambda + 8[1 - \exp(-0.15\eta)] - 0.6 \exp[-(\lambda - 3.1)^2] \quad (\text{Eq. 9-11})$$

C.6.4 Wu et al. [2000]

The Wu et al. (2000) formula applies to both sand and gravel bed streams. The formula computes the suspended and bed load separately and adds them together to obtain the total bed material sediment load:

$$q_t = q_b + q_s \quad (\text{Eq. 9-12})$$

The bed load is computed from:

$$\frac{q_{bi}}{p_i \sqrt{g(s-1)d_i^3}} = 0.0053 \left[\left(\frac{n'}{n} \right)^{1.5} \frac{\tau_b}{\tau_{ci}} - 1 \right]^{2.2} \quad (\text{Eq. 9-13})$$

where $n' = 0.05d_{50}^{1/6}$ and n is total Manning’s roughness coefficient for the bed.

The critical shear stress is computed as:

$$\tau_{ci} = \theta_c (s-1) d_i \xi_i \quad (\text{Eq. 9-14})$$

and the exposure factor, ξ_i , is computed as:

$$\xi_i = \left(\frac{p_{hi}}{p_{ei}} \right)^\alpha \quad (\text{Eq. 9-15})$$

where $\alpha = 0.6$, which can be modified by the user. The probability of hiding and exposure, p_{hi} and p_{ei} respectively, are computed as:

$$p_{hi} = \sum_{j=1}^N \frac{p_j d_j}{(d_i + d_j)}, \quad p_{ei} = \sum_{j=1}^N \frac{p_j d_i}{(d_i + d_j)} \quad (\text{Eq. 9-16})$$

The critical shear stress, θ_c , recommended is 0.03; however, the user can modify this if necessary. The suspended load is computed as:

$$\frac{q_{si}}{p_i \sqrt{g(s-1)d_i^3}} = 0.0000262 \left(\frac{U}{w_{fi}} \left(\frac{\tau_b}{\tau_{ci}} - 1 \right) \right)^{1.74} \quad (\text{Eq. 9-17})$$

C.6.5 Parker's Method [1990]

Parker [1990] developed an empirical gravel transport function based on the equal mobility concept and field data:

$$\frac{q_{bi} g (s-1)}{p_i (\tau_g / \rho)^{1.5}} = 11.93 f(\phi_i) \quad (\text{Eq. 9-18})$$

where q_{bi} = volumetric sediment transport rate per unit width for size fraction i ; τ_g = grain shear stress, d_{50} = the median diameter; g = acceleration of gravity; γ = specific weight of water; and s = relative specific density of sediment (ρ_s / ρ).

The parameter ϕ_i is a measure of the shear stress relative to the reference shear stress:

$$\phi_i = \theta_i / (\xi_i \theta_c) \quad (\text{Eq. 9-19})$$

where θ_c is the reference Shield's number; and θ_i = Shield's parameter of the sediment size class i computed as:

$$\theta_i = \tau_g / (\gamma (s-1) d_i) \quad (\text{Eq. 9-20})$$

where τ_g is the grain shear stress. The grain shear stress is computed based upon the velocity and representative grain diameter:

$$\frac{U}{\sqrt{\tau_g / \rho}} = 2.5 \ln \left(\frac{12.27 R'}{k_s} \right) \quad (\text{Eq. 9-21})$$

where U is the cross sectional average velocity, R' is the hydraulic radius due to grain shear stress ($\tau_g = \gamma R' S_f$). The parameter, k_s , is the grain roughness height computed as, $k_s = 2d_{90}$ as suggested by Parker [1990]. The parameter ξ_i is the exposure factor, which accounts for the reduction in the critical shear stress for relatively large particles and the increase in the critical shear stress for relatively small particles:

$$\xi_i = (d_i/d_{50})^{-\alpha} \quad (\text{Eq. 9-22})$$

where $\alpha =$ a constant. The function, $f(\phi_i)$, was fit to field data and is:

$$f(\phi) = \begin{cases} (1 - 0.853/\phi)^{4.5} & , \phi > 1.59 \\ 0.000183 \exp[14.2(\phi - 1) - 9.28(\phi - 1)^2] & , 1 < \phi \leq 1.59 \\ 0.000183\phi^{14.2} & , \phi \leq 1 \end{cases} \quad (\text{Eq. 9-23})$$

Two parameters can be defined by the user to use Parker's equation: θ_c and α . Ideally, these values should be fit to data of the stream being simulated. However, in the absence of data, several references provide guidance, such as Buffington and Montgomery [1997], Andrews [2000], and Mueller et al. [2005]. Default values for θ_c and α are 0.0386 and 0.905 as recommended in Parker [1990].

C.6.6 Results

The comparison between the measured and computed sand total loads are given in figure C-22 for gage SJB in Reach 2B and figure C-23 for gage MEN in Reach 3. In reach 2B there are only measurements below 1,500 cfs. Both the Engelund and Hansen [1972] and Madden [1993] formulas generally overestimate the sediment loads, while the other three formulas underestimate the loads. Parker [1990] predicts the lowest transport rates, but this is expected because the formula is only intended to compute the bed load portion of the total load.

For gage MEN, there are measurements taken at flows over 3,000 cfs so there is a large range of flows to compare against. Similar to the results at SJB, both Engelund-Hansen [1972] and Madden [1993] overestimate sediment loads for flows below 1,500 cfs, while the other 3 formulas underestimate the load. At flows over 3,000 cfs, all the formulas underestimate the sand load, but Engelund and Hansen [1972] and Madden [1993] are the closest to estimating the correct sand load. On balance, the Engelund and Hansen [1972] formula is considered to be the most reliable transport formula for use for this project, but there will be model sensitivity simulations performed using all the five transport formulas.

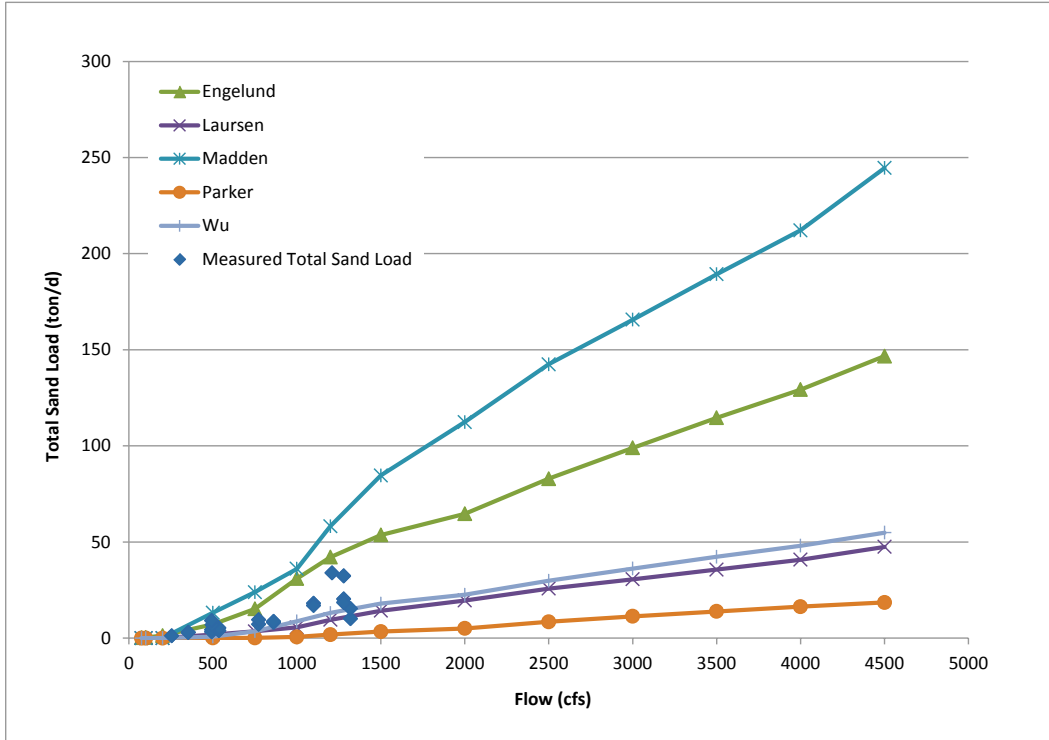


Figure C-22.—Comparison of transport formulas to measured sand load data at SJB.

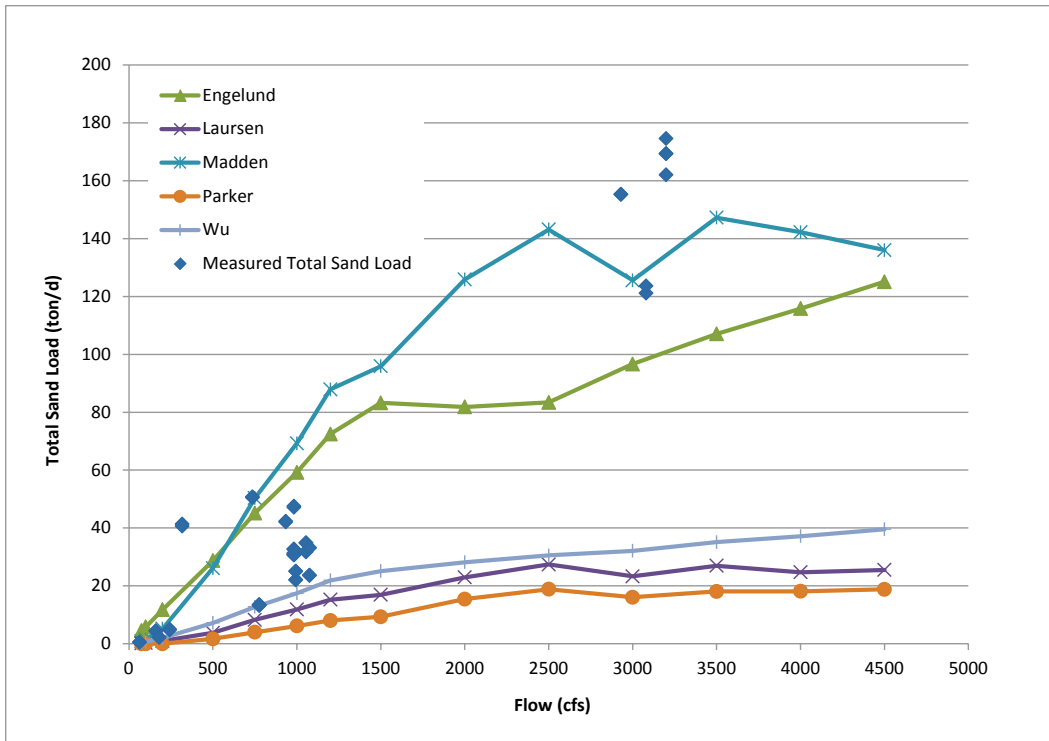


Figure C-23.—Comparison of transport formulas to measured sand load data at MEN.

C.7 Option 1

C.7.1 Bed Elevations

The elevation of the control structure sill at the head of the Bypass was assumed to be 145 ft, which is about 3 to 4 ft lower than the existing channel thalweg elevation at the upstream end of the Bypass channel where it connects to Reach 2B of the SJR. The decrease in elevation will allow restoration flows to significantly incise the river channel in lower Reach 2B. Currently, the channel bed in lower Reach 2B is relatively flat and the low flow channel is relatively wide compared to the upper portion of Reach 2B. The current morphology of the lower Reach 2B is related to deposition within the channel bed caused by backwater from the Mendota Dam. Increasing the slope in the lower portion of Reach 2B will decrease the width of the channel and increase the complexity of the low flow channel over time.

The results of the thalweg profile after a 25 year simulation using SRH-1D for Option 1 and 2 are shown in figure C-24 and figure C-25. The 25 year period is chosen because the river bed is relatively stable after 25 years. The simulation results with subsidence and without subsidence are shown.

For the case of no subsidence, there is approximately 3 to 4 ft of incision at the downstream end of Reach 2B where it connects into the Bypass. The incision gradually decreases until it is approximately zero, about 3.5 miles upstream of the Bypass (station 480,000 or RM 209.7). For the case of subsidence, the region and magnitude of deposition is not significantly different.

There is up to 5 ft of deposition in Reach 3 immediately below the Bypass that gradually decreases to zero deposition, approximately 0.8 miles downstream of the Bypass. Downstream of this, the model is predicting erosion within Reach 3 because despite the additional sediment being supplied from Reach 2B, there is a net deficit of sediment supplied to this reach. Reclamation [2009] also predicted similar amounts of erosion under the SJRRP. Reclamation [2009] used SJRRP projected flows that were similar to those used in this report, and predicted Reach 3 to erode approximately 1 ft on average under baseline conditions and approximately 2 ft on average under SJRRP Conditions.

The erosion in Reach 3 is likely, primarily due to the significant increase in flow in Reach 3 as the result of the SJRRP flows (compare table A-3 to table A-4). The 5 percent exceedance flow increased from approximately 1,300 cfs under pre-SJRRP conditions to over 3,500 cfs under current SJRRP conditions. These are still relatively small flows compared to pre-Friant Conditions, but the levees built since the completion of Friant Dam constrain the flows and increase the sediment transport in the main channel.

There is some uncertainty regarding this deficit because the supply of sand from Fresno Slough has not been measured. To compute the effect of the Fresno Slough, simulations were performed assuming no inflow from Fresno Slough. Without the flows from Fresno Slough, there is about 1 ft more deposition in Reach 3, just downstream of the Bypass (figure c-26). However, there is still erosion predicted 2 miles downstream of the Bypass. Deposition at high flow is also likely within the lower Bypass channel. The backwater of Reach 3 decreases the flow velocities in the lower Bypass at high flows (greater than 1,500 cfs) and sand will likely deposit in the lower Bypass. Later designs may include a narrowing of the floodplain to accelerate the flow in the lower Bypass and to limit the excavation costs.

C.7.2 Sediment Loads

The erosion in lower Reach 2B and the deposition in upper Reach 3 over time are shown in figure C-27. Erosion and deposition occur most rapidly in the first 6 years as the channel adjusts to the new project conditions. By year 15, most of the erosion and deposition that is going to occur has occurred. The channel then enters a dynamic equilibrium when there are alternating periods of small amounts of erosion and deposition. Approximately 470,000 tons of sediment was eroded from Reach 2B during the first 25 years of simulation and approximately 440,000 tons was deposited in the lower Bypass and Reach 3.

The sediment loads at the entrance to the Bypass and approximately 1.5 miles downstream of the Bypass are shown in figure C-28. Within the first 25 years, there is 1.26 million tons of sediment supplied to the upstream end of the Bypass, while approximately 820,000 tons is transported 1.5 miles downstream of the Bypass in Reach 3.

The sediment load entering Reach 2B within the first 25 years is 960,000 tons and approximately 1.2 million tons is transported to the end of Reach 3 (figure C-29).

C.7.3 Water Surface Profiles

The thalweg and water surface elevation at a flow of 1,200 cfs after a 25 year simulation is shown in figure C-30. The water surface is expected to decrease approximately 3 ft at the lower end of Reach 2B at a flow of 1,200 cfs due to the incision into Reach 2B. The change in water surface relative to initial conditions decreases until it is zero about 9 miles upstream of the Bypass (which is just downstream of the Chowchilla Bifurcation structure). The water surface in Reach 3 also decreases despite deposition in the upper end of Reach 3 because Reach 3 is degrading throughout most of the reach.

The thalweg and water surface elevation at a flow of 4,500 cfs after a 25 year simulation is shown in figure C-31. The water surface elevations are approximately 2 ft lower in the lower portion of Reach 2B at the end of the

25 year simulation due to erosion. The water surface in Reach 3 decreases because of the overall degradation in Reach 3 during the 25 year simulation.

The detailed evolution of the channel profile under Option 1 is shown in figure C-32. Incision of up to 4 ft occurs within the first mile upstream of the Bypass control structure within Reach 2B. By year 4, most of the deposition in Reach 3 that will occur has occurred. There is gradual bed lowering in the lower 4 miles of Reach 2B from year 4 to year 25, but the rates are relatively slow and there is generally less than 1 ft of change from year 10 to year 25. The pools between the grade control structures in the Bypass are expected to scour over time because of the relative high velocities in the Bypass. The hydraulic depth within the pools at low flow (approximately 100 cfs) could increase to about 6 ft at year 25. Therefore, it is expected that the velocities in the pools within the Bypass will decrease over time, but the velocities at the grade control structures will remain relatively high.

C.8 Option 2

C.8.1 Channel Bed Elevations

The elevation of the control structure at the head of the Bypass was assumed to be 141.5 ft, about 7 to 8 ft lower than the existing channel thalweg elevation at the upstream end of the Bypass channel, where it connects to Reach 2B of the SJR. The decrease in elevation will allow restoration flows to significantly incise the river channel in the lower portion of Reach 2B. The elevation of the upstream end of the Bypass was set to establish an approximately uniform slope through Reach 2B and the Bypass. Currently, the channel bed in the lower portion of Reach 2B is relatively flat and the low flow channel is relatively wide compared to the upper portion of Reach 2B. Increasing the slope in the lower portion of Reach 2B will decrease the width of the channel and increase the complexity of the low flow channel over time.

The results of the thalweg profile after a 25 year simulation using SRH-1D for Option 1 and 2 are shown in figure C-24 and figure C-25. Results with subsidence and without subsidence are shown.

For the case of no subsidence there is approximately 7 to 8 ft of incision at the downstream end of Reach 2B where it connects into the Bypass. The incision gradually decreases until it is approximately zero about 4 miles upstream of the Bypass (RM 210.2). For the case of subsidence the region and magnitude of deposition is not significantly different.

There is up to 7 ft of deposition in Reach 3 immediately below the Bypass that gradually decreases to zero deposition approximately 1 mile downstream of the Bypass. Downstream of this, the model is predicting erosion within Reach 3 because despite the additional sediment being supplied from Reach 2B, there is a

net deficit of sediment supplied to this reach. There is some uncertainty regarding this deficit because the supply of sand from Fresno Slough has not been measured.

The Bypass is expected to erode 1 to 2 ft because the overall trend in Reach 3 is erosional and the erosion may progress into the Bypass. The erosion in the Bypass is a primary reason why grade control is suggested in the lower portion of the Bypass. As mentioned previously, there is some uncertainty regarding the sediment supply to Reach 3 and therefore the extent of the erosion in Reach 3 is uncertain. The sensitivity of the model to flows entering from Delta-Mendota Canal and from Fresno Slough was investigated by simulating the same period of time with zero inflow from these sources. The simulated bed profile after 25 years is shown in figure C-26. The bed in Reach 3 is approximately 1 to 1.5 ft higher under this scenario than under the previous simulation. The Bypass profile shows less incision and the bed of the Bypass remains relatively stable under this scenario.

The differences in the river bed elevations between Option 1 and 2 are local and are not expected to extend beyond approximately 4 miles upstream of the Bypass and 2 miles downstream of the Bypass.

C.8.2 Sediment Loads

The erosion in lower Reach 2B and the deposition in upper Reach 3 over time are shown in figure C-27. Erosion and deposition occur most rapidly in the first 6 years as the channel adjusts to the new project conditions. By year 15, most of the deposition in Reach 3 that is going to occur has occurred, but the erosion in Reach 2B continues at slow rates until the end of the simulation. There is approximately 660,000 tons of erosion predicted within Reach 2B during the first 25 years of simulation. There is approximately 580,000 tons of deposition predicted within the lower Bypass and Reach 3.

The sediment loads at the entrance to the Bypass and approximately 1.5 miles downstream of the Bypass are shown in figure C-28.

Options 1 and 2 have nearly identical sediment loads entering Reach 2B and exiting Reach 3 (figure C-29).

C.8.3 Water Surface Elevations

The thalweg and water surface elevation at a flow of 1,200 cfs after a 25 year simulation is shown in figure C-30. The water surface is expected to decrease approximately 5 ft at the lower end of Reach 2B at a flow of 1,200 cfs due to the incision into Reach 2B. The change in water surface relative to initial conditions decreases until it is zero about 9 miles upstream of the Bypass (RM 214). The water surface in Reach 3 also decreases despite deposition in the upper end of Reach 3 because Reach 3 is degrading throughout most of the reach.

The thalweg and water surface elevation at a flow of 4,500 cfs after a 25 year simulation is shown in figure C-31. The water surface elevations are approximately 3 ft lower in the lower portion of Reach 2B at the end of the 25 year simulation due to erosion. The water surface in Reach 3 decreases because of the overall degradation in Reach 3 during the 25 year simulation.

The detailed evolution of the channel profile under Option 2 is shown in figure C-33. Incision of up to 7 ft occurs within the first mile upstream of the Bypass control structure within Reach 2B. By year 4, most of the deposition in Reach 3 that will occur has occurred. There is gradual bed lowering in the lower 4 miles of Reach 2B from year 4 to year 25, but the rates are relatively slow and there is generally less than 1 ft of change from year 10 to year 25. The pools between the grade control structures in the Bypass are expected to scour over time because of the relative high velocities in the Bypass. The hydraulic depth within the pools at low flow could increase to about 6 ft at year 25. Therefore, it is expected that the velocities in the pools within the Bypass will decrease over time, but the velocities at the grade control structures will remain relatively high.

C.9 Impacts to Floodplain Habitat in Reach 2B

The decrease in river bed and water surface elevations in Reach 2B after flows are introduced into the Bypass for both Options 1 and 2 will decrease the area of inundation in Reach 2B. This section describes the previous estimates of inundation and then proposes a floodplain grading plan to increase the amount of inundation under Option 2. There is no floodplain grading plan developed for Option 1 because Option 2 is assumed to be the preferred option. The volume of floodplain grading is expected to be less under Option 1.

C.9.1 Previous Estimate

The previous estimates for inundated area for two alternative levee alignments, FP2 and FP4, as described in the Reach 2B Project Description are given in table C-6 [SJRRP 2012b]. The actual preferred levee alignment in Reach 2B is generally between FP2 and FP4 because of specific landowner agreements. These estimates assumed no incision of the bed in Reach 2B. In addition, the assumed sill elevation for the compact Bypass flow control structure was 148 ft, and there was no mobile bed simulation that estimated future bed elevation changes as a result of the project.

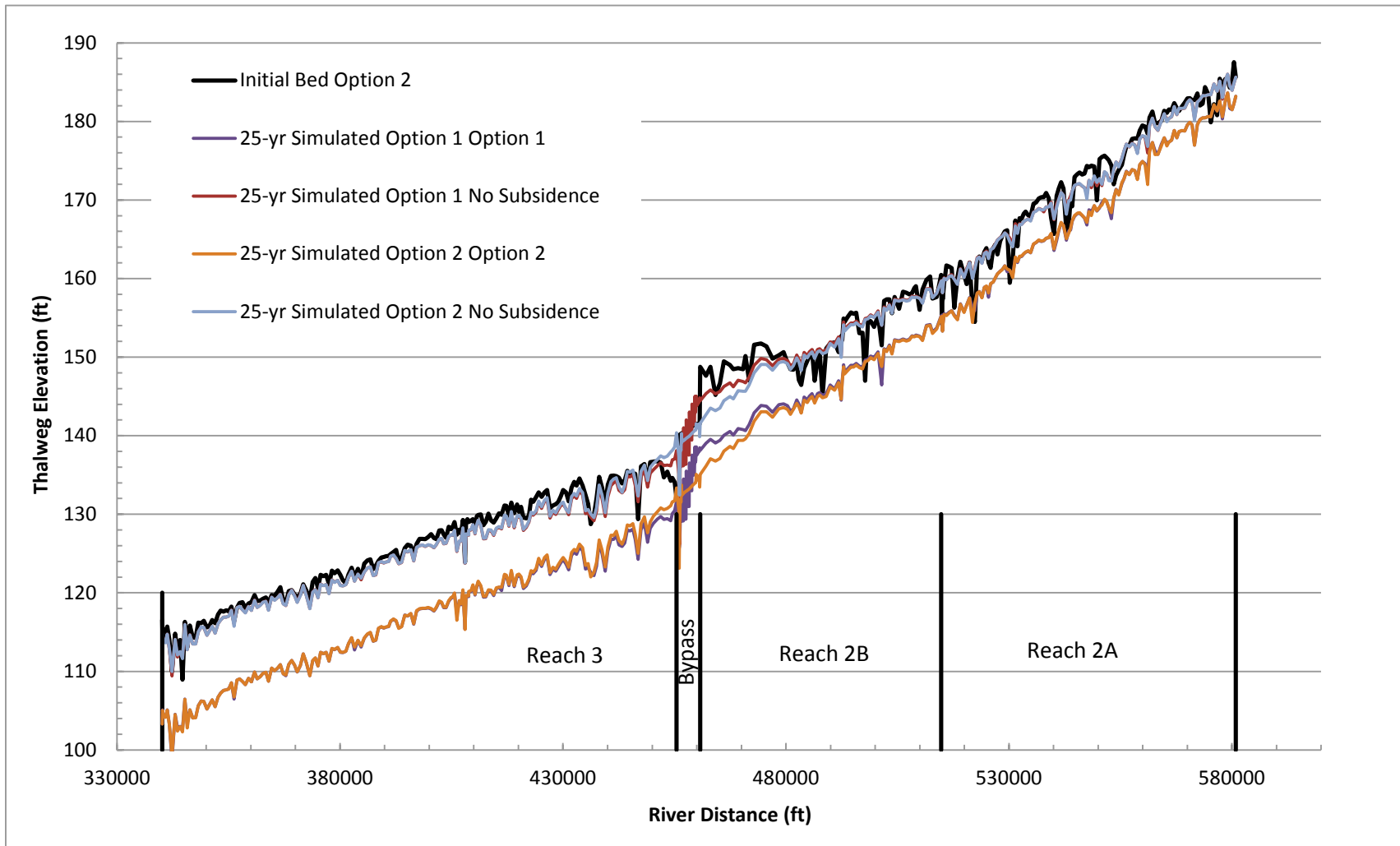


Figure C-24.—Initial and 25 year simulated thalweg elevation for Reach 2A through Reach 3. For both Options 1 and 2, the bed elevation is impacted within the first 4 miles upstream from the Bypass and within the first mile downstream of the Bypass.

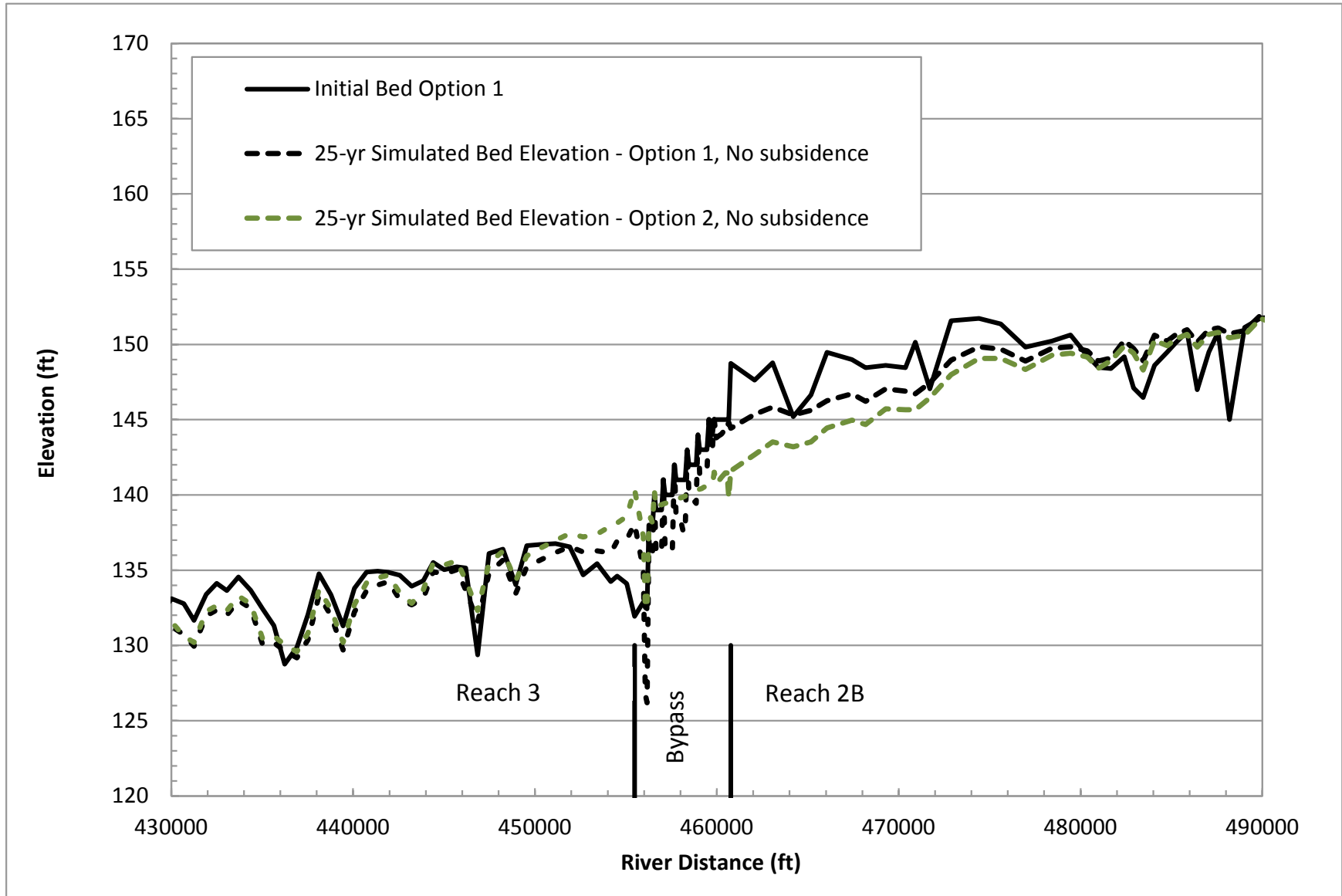


Figure C-25.—Initial and 25 year simulated thalweg elevation in vicinity of compact Bypass.

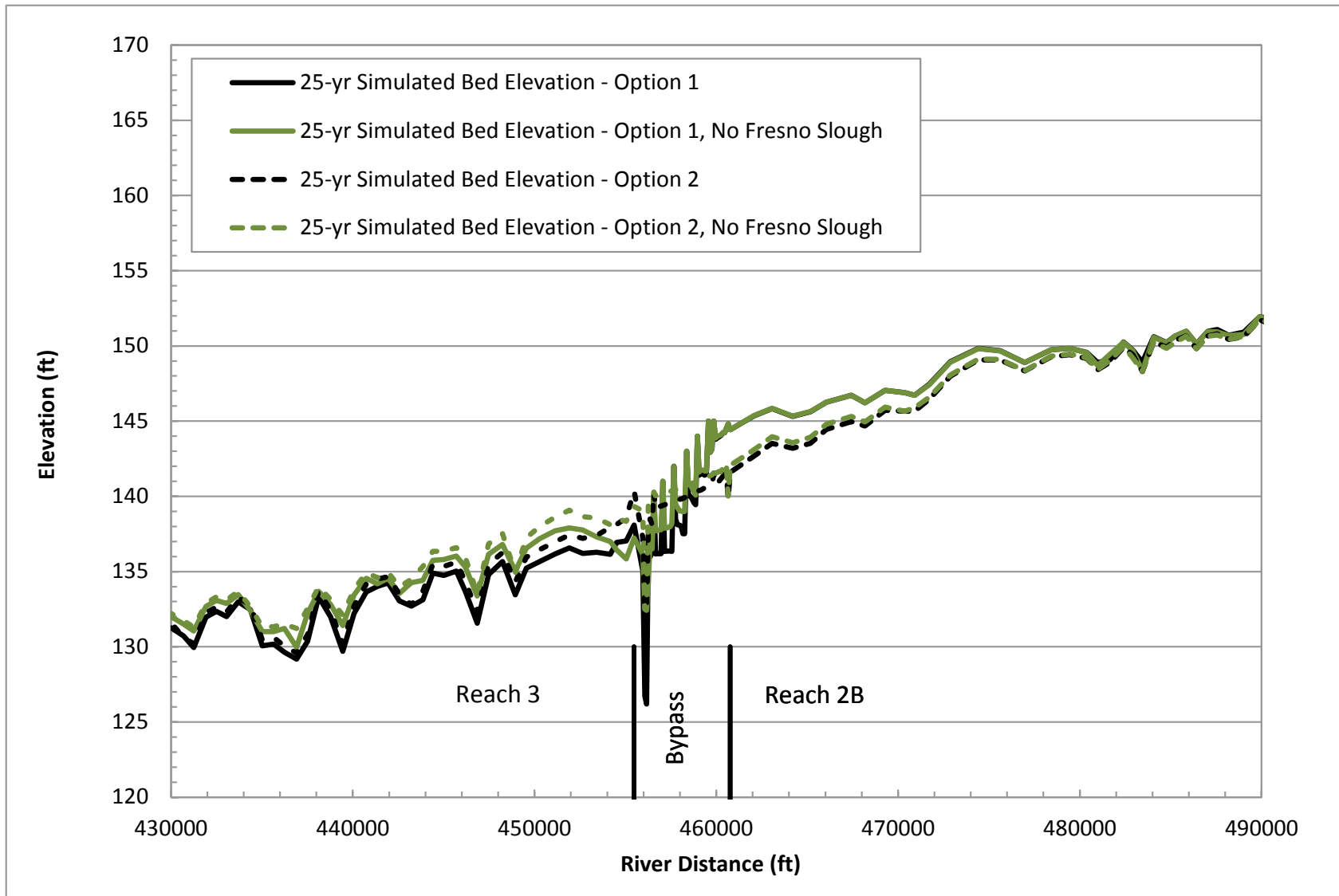


Figure C-26.—Initial and 25 year simulated thalweg elevation in vicinity of compact Bypass, with and without inflows from the Fresno Slough for Options 1 and 2.

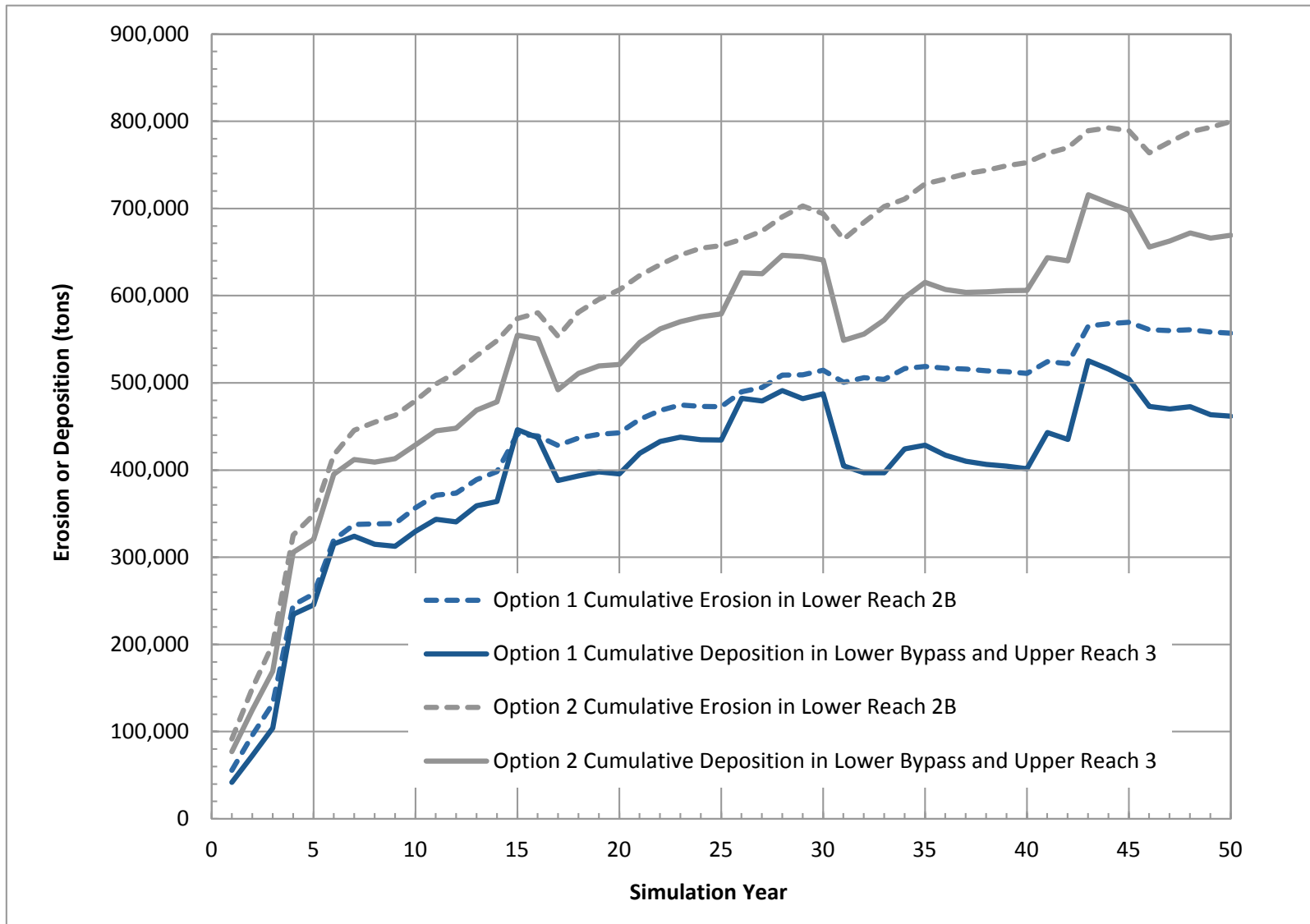


Figure C-27.—Simulated erosion in Reach 2B and deposition in Reach 3 within 50 year period for Option 1 and 2 without subsidence.

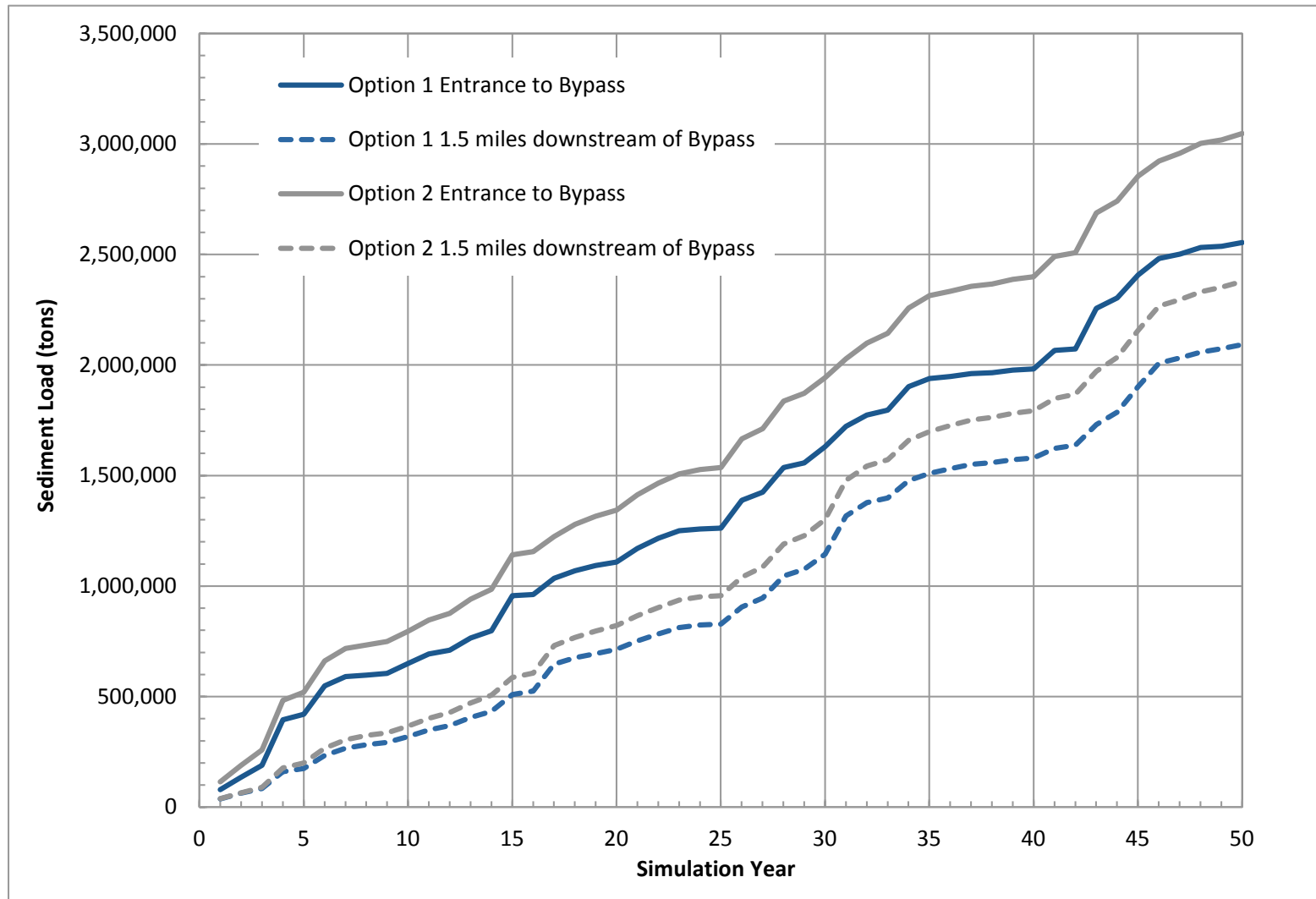


Figure C-28.—Simulated sediment loads within 50 year period for Option 1 and 2 without subsidence.

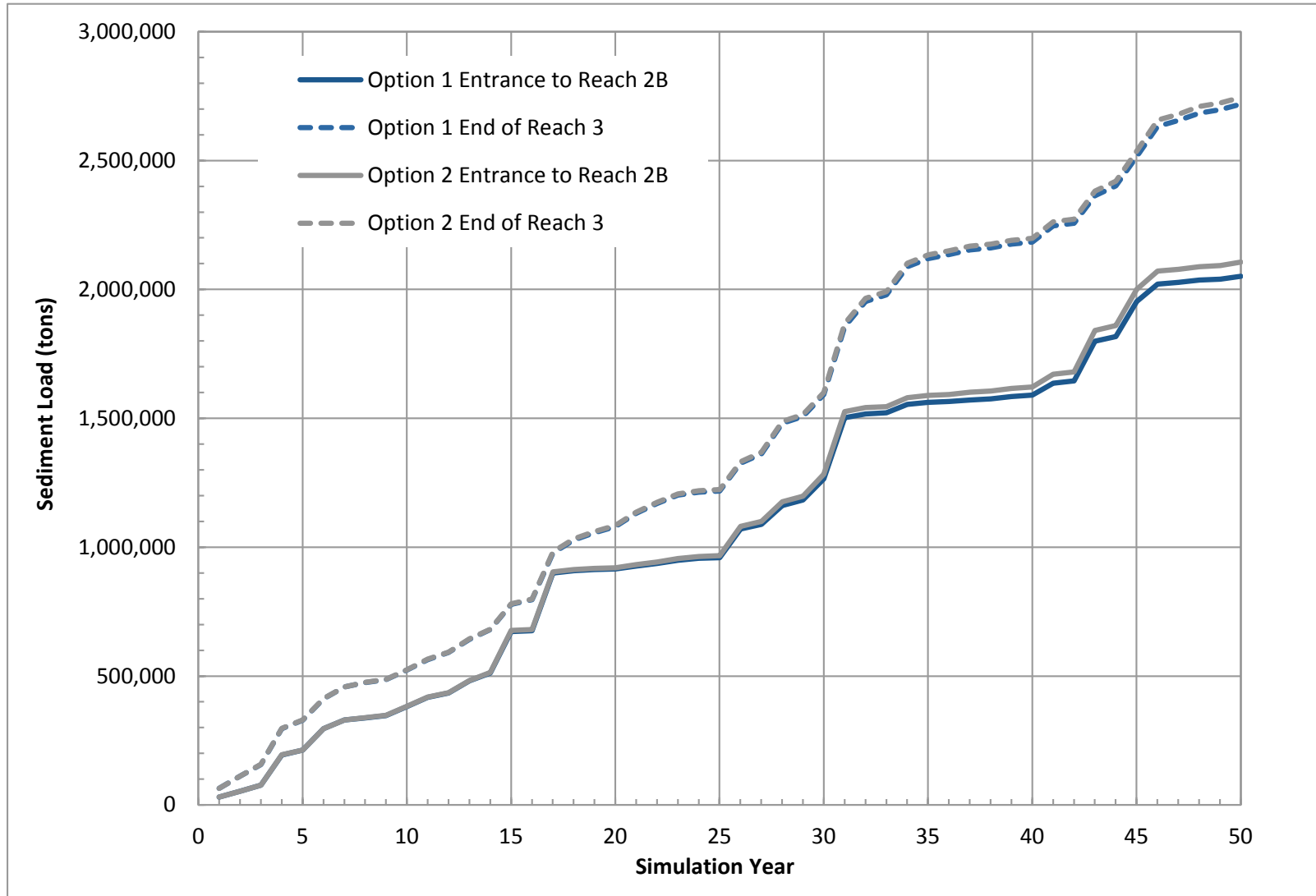


Figure C-29. Simulated sediment loads at upstream end of Reach 2B and downstream end of Reach 3 within 50 year period for Option 1 and 2 without subsidence.

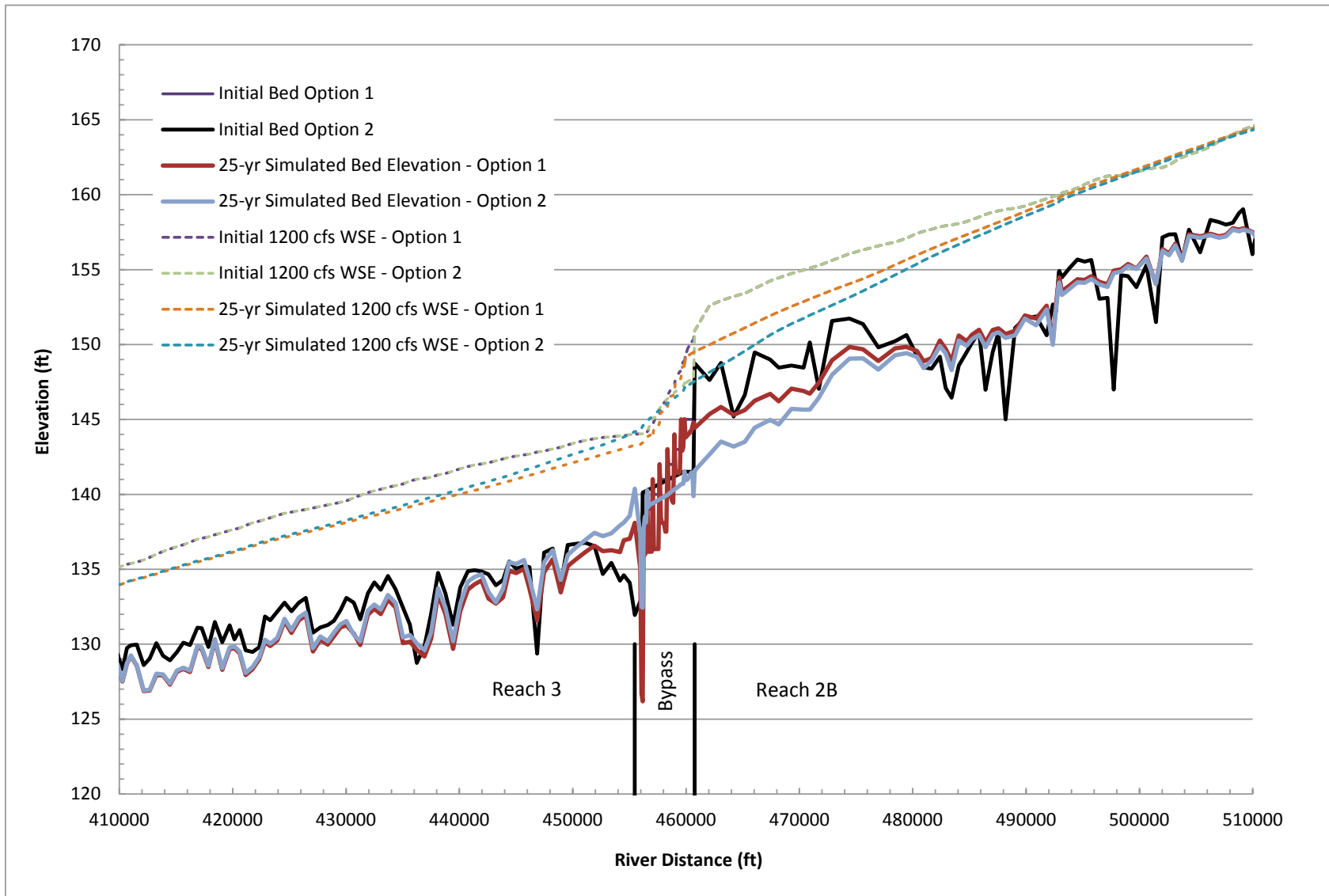


Figure C-30.—Thalweg elevation and water surface elevation at a flow of 1,200 cfs for Option 1 and 2 after a 25 year SRH-1D simulation without subsidence. The initial water surface elevation and bed elevations in Reach 3 and 2B are almost identical between Option 1 and 2.

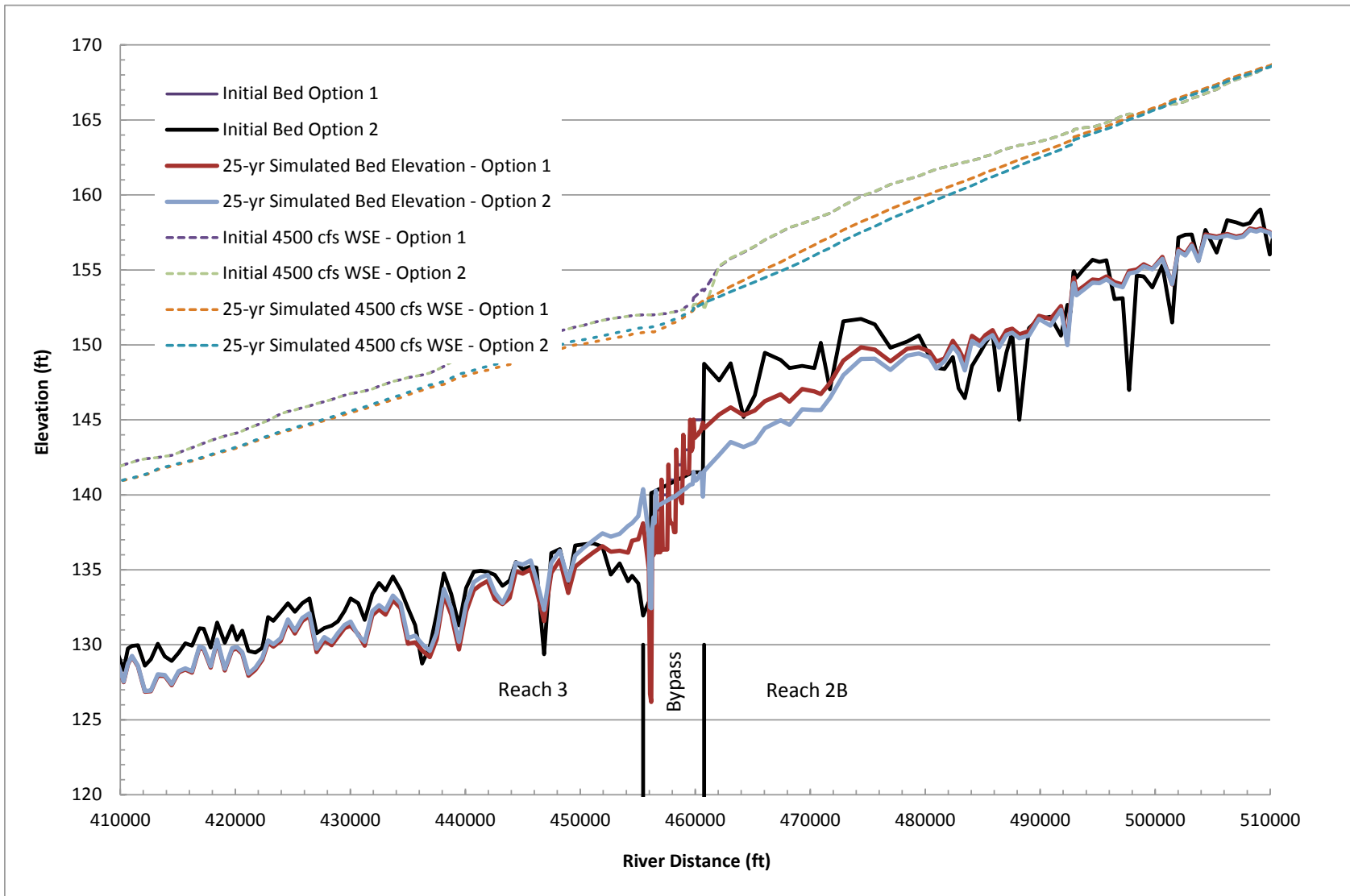


Figure C-31.—Thalweg elevation and water surface elevation at a flow of 4,500 cfs for Option 1 and 2 after a 25 year SRH-1D simulation without subsidence. The initial water surface elevation and bed elevations in Reach 3 and 2B are almost identical between Option 1 and 2.

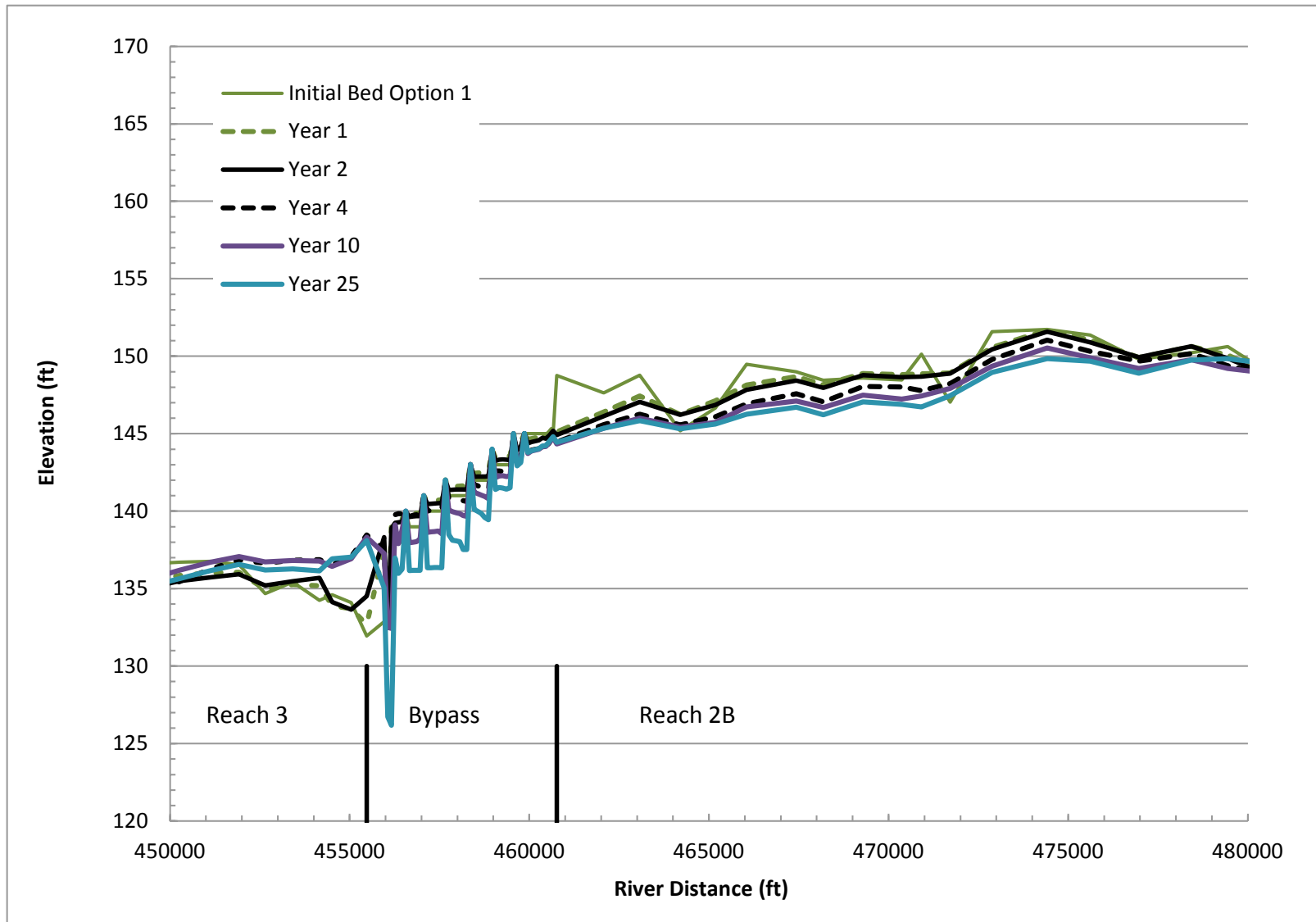


Figure C-32.—Thalweg elevation for Option 1 for various years after construction.

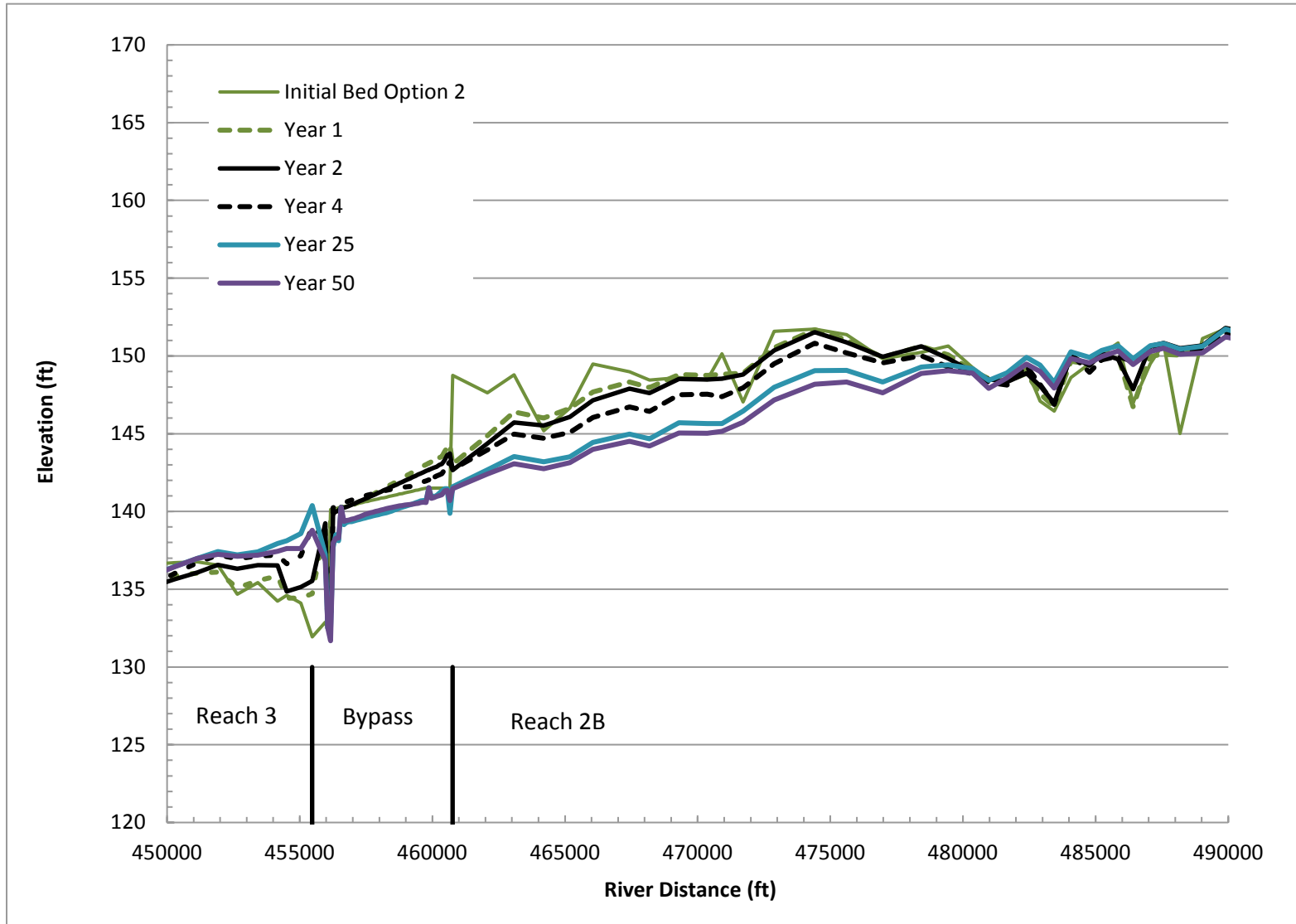


Figure C-33.—Thalweg elevation for Option 2 for various years after construction.

C.9 Impacts to Floodplain Habitat in Reach 2B

The decrease in river bed and water surface elevations in Reach 2B after flows are introduced into the Bypass for both Options 1 and 2 will decrease the area of inundation in Reach 2B. This section describes the previous estimates of inundation and then proposes a floodplain grading plan to increase the amount of inundation under Option 2. There is no floodplain grading plan developed for Option 1 because Option 2 is assumed to be the preferred option. The volume of floodplain grading is expected to be less under Option 1.

C.9.1 Previous Estimate

The previous estimates for inundated area for two alternative levee alignments, FP2 and FP4, as described in the Reach 2B Project Description are given in table C-6 [SJRRP 2012b]. The actual preferred levee alignment in Reach 2B is generally between FP2 and FP4 because of specific landowner agreements. These estimates assumed no incision of the bed in Reach 2B. In addition, the assumed sill elevation for the compact Bypass flow control structure was 148 ft, and there was no mobile bed simulation that estimated future bed elevation changes as a result of the project.

Table C-6.—Previous Estimated Inundated Area for FP2 and FP4 Levee Setbacks in Reach 2B [from SJRRP 2012b] Assuming Existing Bed Geometry

| Flow (cfs) | Total Inundated Area (acres) | |
|------------|------------------------------|-------|
| | FP2 | FP4 |
| 1,000 | 356 | 416 |
| 1,500 | 662 | 853 |
| 2,000 | 997 | 1,323 |
| 2,500 | 1,170 | 1,526 |
| 3,000 | 1,242 | 1,643 |
| 3,500 | 1,275 | 1,702 |
| 4,000 | 1,308 | 1,762 |
| 4,500 | 1,323 | 1,800 |

The Minimum Floodplain Habitat Report [SJRRP, 2012c] estimated the amount of suitable inundated habitat necessary to support a self sustaining population of salmon and the existing amount of suitable inundation. The method for estimating existing Area of Suitable Habitat (*ASH*) for juvenile salmon relies on estimate of both hydraulic suitability and cover suitability. At each grid cell within the selected subportions of each reach and for each flow, a habitat suitability index (*HSI*) ranging from 0 to 1 was assigned to each variable (depth, velocity, and cover), from which a total *HSI* was computed at each grid cell. The total habitat suitability index (HSI_T) of each grid cell was computed as the minimum of the individual *HSI* values:

$$HSI_T = \min(HSI_D, HSI_V, HSI_C) \quad (\text{Eq. 9-24})$$

where HSI_T = total habitat suitability of the grid cell
 HSI_D = depth habitat suitability of the grid cell
 HSI_V = velocity habitat suitability of the grid cell
 HSI_C = cover habitat suitability of the grid cell

ASH was calculated as the sum over all the grid cells of the inundated cell area multiplied by HSI_T for that grid cell:

$$ASH = \sum_{i=1}^N TIA_i \cdot HSI_{T,i} \quad (\text{Eq. 9-25})$$

where ASH = area of suitable habitat
 TIA_i = inundated area within the grid cell i
 $HSI_{T,i}$ = total habitat suitability of the grid cell i
 N = number of grid cells within simulation domain

Fish observations from the Stanislaus River, a tributary of the SJR, were used as the basis for depth and velocity hydraulic habitat suitability [Aceituno, 1990] (figure C-34). The cover suitability is defined based upon vegetation and the presence of edge type features (table C-7).

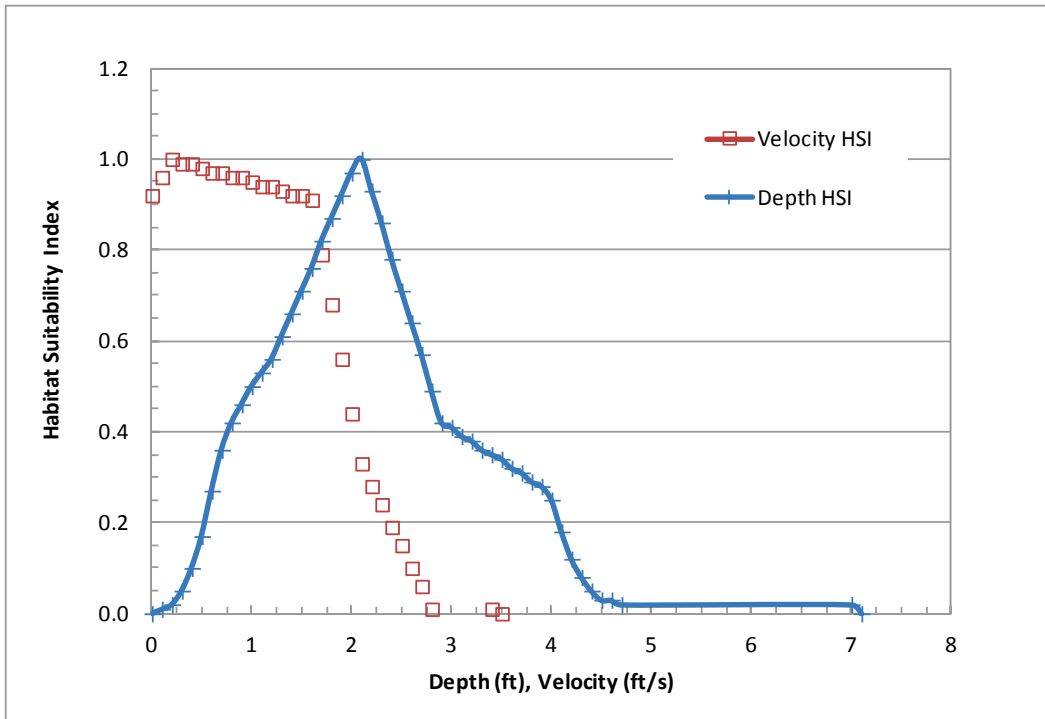


Figure C-34.—Habitat Suitability Index values as a function of depth and velocity from Stanislaus River [Aceituno, 1990].

Table C-7.—Cover *HSI* Scores Assumed in Reclamation [2012d].

| Cover Type | Assumed HSI Value |
|----------------------------------|-------------------|
| No Cover, River Wash | 0.07 |
| Gravel Bars | 0.28 |
| Grass, Herbaceous | 0.49 |
| Willow Riparian and Willow Scrub | 0.80 |
| Wetland/Marsh | 0.60 |
| Edge Habitat | 1.00 |

Using the above assumptions on *HSI*, Reclamation [2012d] estimated the available *ASH* and the results are given in table C-8. The maximum fraction of suitable habitat relative to total inundation occurred in Reach 4B2, and was approximately computed as 0.24 to 0.28 for flows between 1,225 cfs and 3,655 cfs. The fraction of hydraulically suitable area (which is defined as the suitable area ignoring the cover suitability criteria) was 0.29 to 0.31 for these same flows. Reach 4B2 is considered to be perhaps the best analog for Reach 2B after levee setback, floodplain regarding and revegetation.

Table C-8.—Estimates of Existing Inundation and Suitable Juvenile Salmon Rearing Habitat in the SJRRP Reaches [Reclamation, 2012d]

| Reach | Flow (cfs) | Total Inundation (acres) | Fraction Hydraulically Suitable (-) | Fraction Suitable (-) |
|--------------------------|------------|--------------------------|-------------------------------------|-----------------------|
| Dry Water Year | | | | |
| 1B | 1,500 | 668 | 0.25 | 0.10 |
| 2A | 1,375 | 625 | 0.33 | 0.15 |
| 3 | 1,225 | 495 | 0.18 | 0.09 |
| 4A | 1,225 | 359 | 0.22 | 0.14 |
| 4B2 | 1,225 | 713 | 0.29 | 0.28 |
| Normal Water Year | | | | |
| 1B | 2,500 | 798 | 0.23 | 0.07 |
| 2A | 2,355 | 743 | 0.29 | 0.14 |
| 3 | 2,180 | 770 | 0.23 | 0.08 |
| 4A | 2,180 | 427 | 0.19 | 0.13 |
| 4B2 | 2,180 | 1041 | 0.29 | 0.27 |
| Wet Water Year | | | | |
| 1B | 4,000 | 982 | 0.2 | 0.06 |
| 2A | 3,855 | 876 | 0.25 | 0.13 |
| 3 | 3,655 | 1015 | 0.23 | 0.07 |
| 4A | 3,655 | 525 | 0.16 | 0.13 |
| 4B2 | 3,655 | 1432 | 0.31 | 0.24 |

The Minimum Floodplain Habitat Report [SJRRP, 2012c] estimated that 144 acres of suitable juvenile salmon habitat is necessary in Reach 2B. More would be required in Reach 2B if the habitat deficits of Reaches 1B, 2A, and 3 were included into the habitat needs of Reach 2B.

C.9.2 Inundation under Option 2

To estimate the inundation under Option 2, a range of steady flows was simulated in Reach 2B using Sedimentation and River Hydraulics – Two-Dimensional (SRH-2D). SRH-2D [Lai, 2008] is a depth averaged 2D hydraulic model that can simulate the depth and velocity within a user-defined unstructured grid. The main inputs into the model include: geometry, roughness, and boundary conditions. Each input is described below.

C.9.2.1 Geometry

Terrestrial geometry is comprised of the above water and below water ground elevations in the vicinity of the river, floodplain, and levees. For this study, 2008 aerial Light Detection and Ranging (LiDAR) was used to define the topography over the study reach, acquired by the California Department of Water Resources. Horizontal and vertical datums of the LiDAR data are North American Datum of 1983 (NAD83) and the North American Vertical Datum of 1988 (NAVD88), respectively. The geographical coordinates are in the California State plane system, Zone III, in units of U.S. Survey Feet. Separate boat surveys using Sound Navigation and Ranging (SONAR) were performed between 2009 and 2011 to obtain the below water geometry of the stream channel. The projection and datums of the bathymetric surveys match those of the 2008 airborne LiDAR.

The existing terrestrial geometry was modified in three steps:

- The existing stream channel erodes as predicted by SRH-1D. The cross sections from SRH-1D were exported into ArcGIS and the surface was interpolated between them.
- The existing levees are removed and replaced with levees as specified under the preferred levee alignment for Reach 2B. This is estimated to require up to 800,000 cubic yards of excavation.
- Floodplain grading in Reach 2B, the basis for the floodplain grading and preliminary conceptual design, is given below.

Section 2.2 – Rearing Habitat Objectives form the basis for the floodplain and channel grading design. In addition to the objective for the rearing habitat objectives, the following objectives were added.

- Design features, such as side channels, high flow channels, and sloughs, should have analogs within the current or historical (pre-Friant) SJR.
- Design features should encourage active river process in the future.
- Design features should increase ability of river to sustain riparian habitat through active river process.

- Design features should decrease structural constraints on natural river process.

The following design features are used to meet the above design objectives. The description of each feature and their relevance to the SJR are described below. The main strategy is to design sustainable geomorphic features that meet the above objectives. The intention is not to design a static system, but to create a design in which natural geomorphic processes are activated.

- **Low/Split Flow Channels.**—These channels will begin inundation between 50 and 200 cfs, with most beginning inundation at 100 cfs. They will be approximately 10 to 50 ft wide and they will be vegetated with riparian buffer a minimum of about 50 ft wide. There may be large wood features at the head of flow splits and throughout the side channels. A low flow channel is defined as a channel that is only intended to convey a relatively small portion of the low flow, whereas a split flow channel is intended to convey a large portion (more than 1/3) of the low flow. Examples of split and low flow channels are given in figure C-35 and figure C-36.
- **Backwater Areas and Sloughs.**—These features mimic abandoned channels and oxbows. Areas of depressed elevation may or may not be wet and may or may not be connected, but are sufficiently low enough to sustain riparian vegetation. Connected areas provide locations for fish refugia, and disconnected areas provide locations for food production and habitat for other terrestrial species. These areas are expected to accumulate some sediment, but will likely remain depressed areas with riparian vegetation. These may be wide shallow features. Parts of the slough will become connected to the main channel at flows between 0 and 150 cfs; however, some sloughs may also be designed not to activate until about 1,000 cfs. They will be vegetated with a mixture of wetland and woody riparian species. These sloughs can create both permanent and seasonal backwater habitat. An example backwater area is given in figure C-36 and figure C-37.
- **Point Bar Grading.**—Several large-scale point bars were destroyed or minimized when the levees were built and the adjacent lands were leveled for agriculture. These features will create transitional zones between the base flow channel and floodplain. Example point bars are given in figure C-38.
- **High Flow Channels.**—The main purposes of these features are to provide depressions in the floodplain where riparian vegetation will grow and to provide floodplain connection at high flows. Most of the high flow channel features were plowed over by the agricultural development. These features were designed to perform similarly to high flow channels

in less-impacted systems as evidenced through historical photographs. Often the downstream end of the high flow channel will be connected to a backwater slough that will be inundated at all flows and is designed to maintain a continuous connection with the river. The high flow channel is most often intended to activate between 750 cfs and 2,200 cfs. The high flow channel will be vegetated with sparse to medium density woody riparian species to increase roughness and provide cover for fish. Some LWD may also be left in the channels to provide immediate roughness. In locations considered potential risk for channel avulsion, LWD may be placed at the entrance of the high flow side channel to prevent short-term channel avulsions. High flow channels will be sloped in a way to reduce the potential for stranding. An example high flow channel in 1937 is given in figure C-38 and figure C-39.

A conceptual level design using the above features was created that required 1.65 million cubic yards of floodplain excavation. A plan view of the design is given in figure C-40. The flood channels were generally excavated so that they met the depth and velocity suitability criteria of juvenile salmon for flows of 1,200 cfs and above. The flood channels were generally between 75 and 150 ft wide and the depth of excavation varied between 3 to 6 ft. The low flow channels were generally 25 to 50 ft wide and the depth of cut was between 5 to 9 ft.

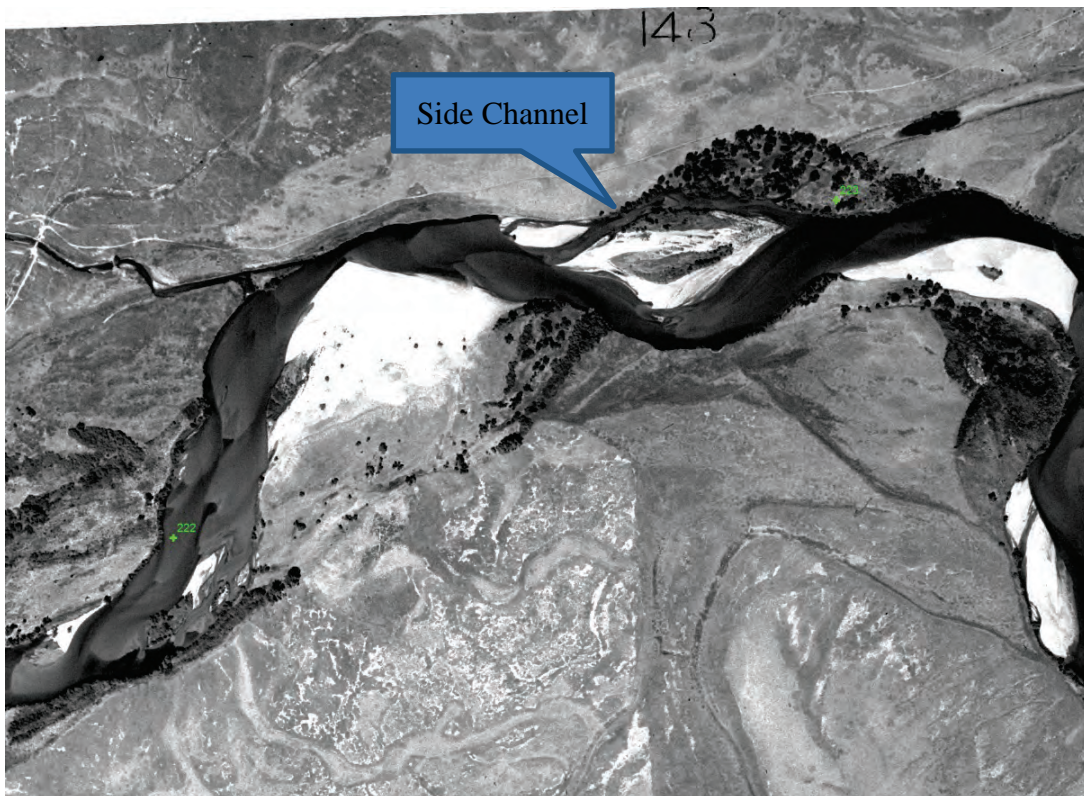


Figure C-35.—Side channel in Reach 2A.



Figure C-36.—Examples of split/side flow channels and a backwater slough in Reach 2A at RM 221 to 220. Aerial photograph in 2011.



Figure C-37.—Reach 3 slough example in 1937 aerial photograph.

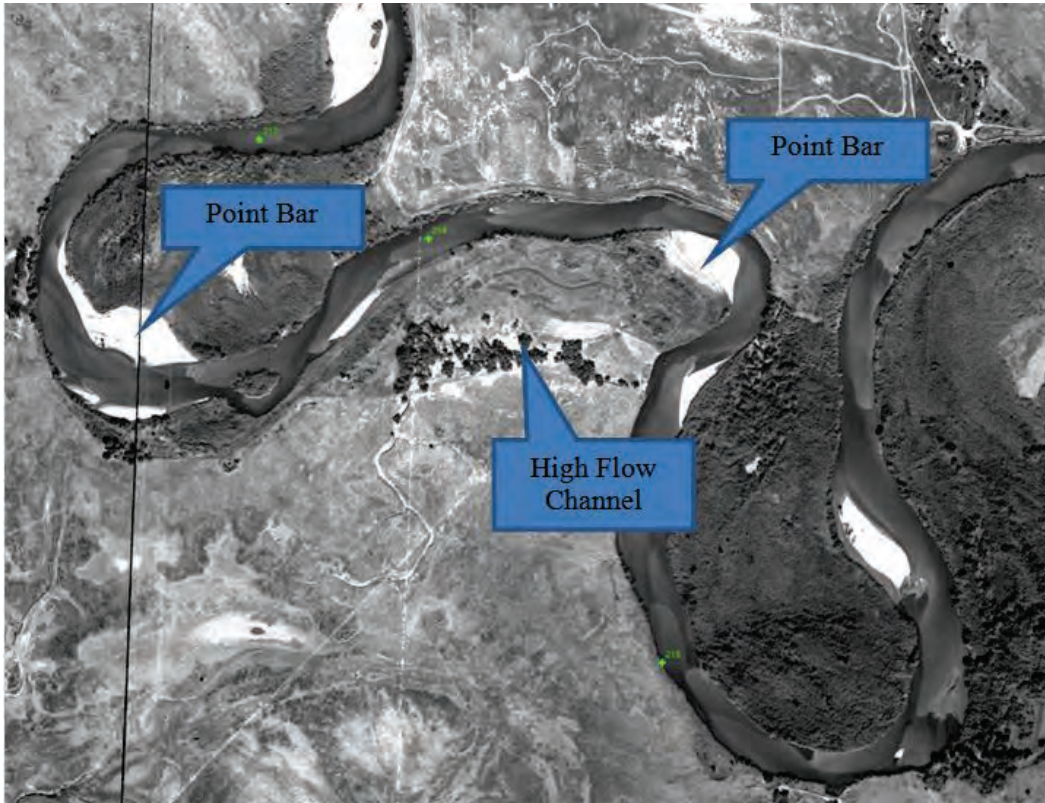


Figure C-38.—High flow channel and point bars in Reach 2B in 1937 aerial photograph.

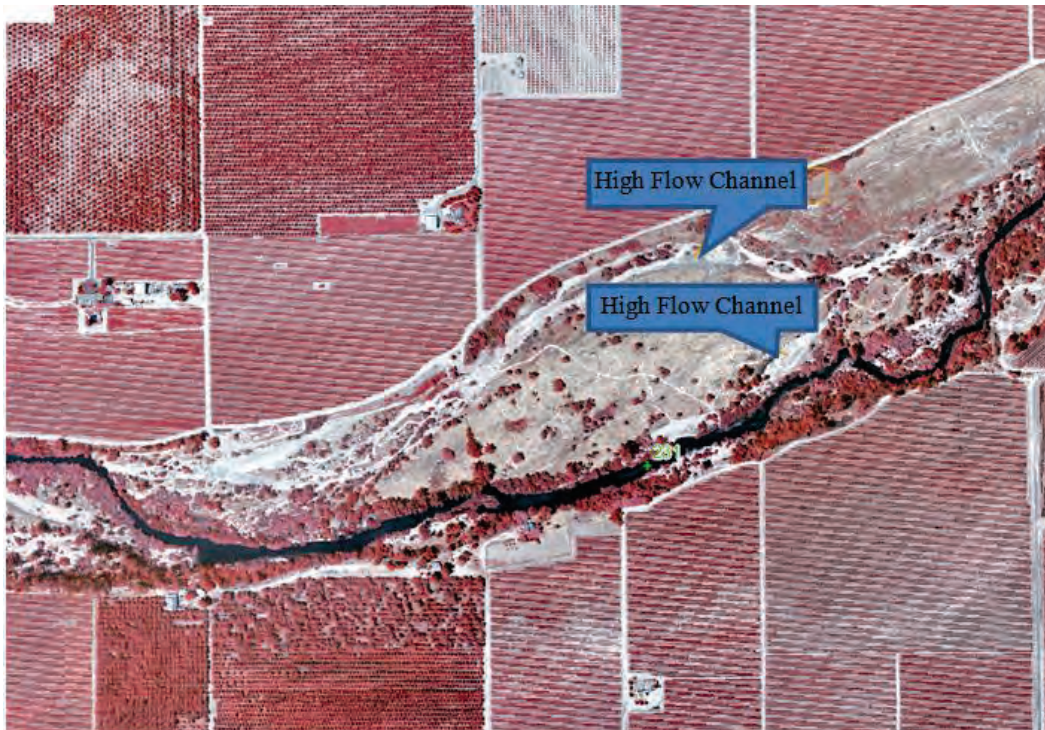


Figure C-39.—Examples of high flow channels in Reach 1B at RM 231 in 2011 aerial photograph.

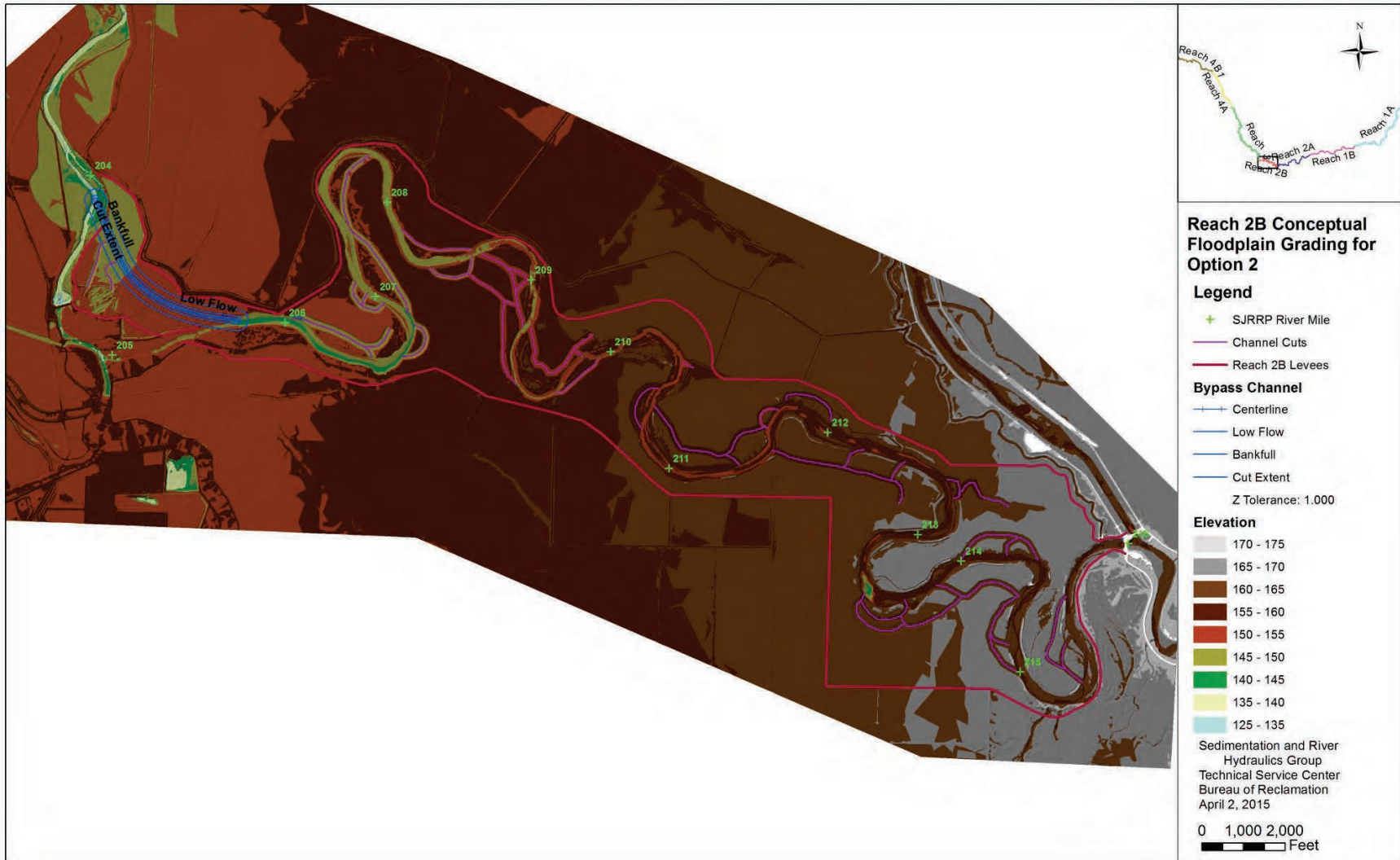


Figure C-40.—Floodplain grading assumed to estimate floodplain inundation for Option 2.

C.9.2.2 Roughness

The roughness values used in this analysis were similar to those used in the analysis of floodplain inundation in Reclamation [2012d]. The agriculture land between the proposed levees was assumed to be converted to light vegetation. The existing riparian corridor between the existing levees was assumed to be a combination of heavy and light vegetation.

Table C-9.—Assumed Roughness Values in SRH-2D for Reach 2B.

| Land Use | Manning's Roughness Values |
|------------------|----------------------------|
| Channel | 0.035 |
| Heavy Vegetation | 0.15 |
| Light Vegetation | 0.06 |
| Top of Levee | 0.035 |

C.9.2.3 Boundary Conditions

The boundary condition used in the model was taken from the computed rating curve at the entrance to the compact Bypass after the SRH-1D model simulated 25 years of sediment transport. The HEC-RAS cross section was 460762.

Table C-10.—Downstream Boundary Condition Used in SRH-2D, Located at Approximate Location of Where Compact Bypass Begins (HEC-RAS cross section 460762)

| Flow (cfs) | Water Surface Elevation (ft) |
|------------|------------------------------|
| 0 | 141.59 |
| 50 | 143.62 |
| 75 | 143.83 |
| 100 | 144.02 |
| 200 | 144.64 |
| 500 | 145.91 |
| 750 | 146.64 |
| 1,000 | 147.18 |
| 1,200 | 147.57 |
| 1,500 | 148.13 |
| 2,000 | 149.06 |
| 2,500 | 149.87 |
| 3,000 | 150.69 |
| 3,500 | 151.40 |
| 4,000 | 152.11 |
| 4,500 | 152.82 |

C.9.2.4 Results

After modification of the existing terrain, SRH-2D was used to simulate the depth of inundation under Option 2 at the various flow rates given in table C-11. The total inundation area, the inundation area less than 1 ft depth, the inundation area greater than 1 ft depth, the area of hydraulically suitable habitat, and the fraction of the total inundated area that is considered hydraulically suitable are all given in the table.

The total inundated area at a flow of 1,000 cfs is actually greater than previous estimates given in table C-6 because of the few low flow channels and slough created by the grading. However, the inundation at 2,000 cfs is significantly less than previous estimates because of the incision into the lower portion of Reach 2B.

The hydraulically suitable area was computed as described in section C.9.1, where the total inundated area at a given grid cell is multiplied by the minimum of the depth and velocity *HSI* to compute the hydraulically suitable area at that grid cell. This procedure is repeated for all the grid cells to compute the hydraulically suitable area (table C-11).

The fraction of hydraulically suitable area is defined as the hydraulically suitable area divided by the total inundated area. The fraction of hydraulically suitable habitat is similar to previous analysis of Reclamation [2012d] in which the fraction of hydraulically suitable habitat of Reach 4B2 was 0.29 to 0.31 for flows between 1,200 cfs and 3,600 cfs.

The revegetation strategy for Reach 2B has not been designed and consequently it is difficult to accurately estimate the effect that cover will have on the fraction of suitable habitat. In Reach B2, the ratio of suitable habitat to hydraulically suitable habitat varied between 0.96 at a flow of 1,225 cfs to 0.77 at a flow of 3,655 cfs. It is expected that the same approximate relation may exist in Reach 2B after the floodplain grading and revegetation implementation. The total suitable area in table C-11 reflects these assumptions.

The above SRH-2D simulations only included Reach 2B and not the Bypass. The total inundation in the Bypass as computed by HEC-RAS at various flows is given in table C-12. The fraction of suitable area is not computed in the Bypass because 2 flow results are not yet available.

Table C-11.—Estimated Inundation in Reach 2B under Option 2. Results Assume Preferred Levee Alignment and Similar Cover *HSI* as in Reach 4B2

| Flow (cfs) | Total Inundated Area (acres) | Inundated Area < 1 ft Depth (acres) | Inundated Area > 1 ft Depth (acres) | Fraction Hydraulically Suitable (-) | Fraction Suitable (-) | Suitable Habitat Area (acres) |
|------------|------------------------------|-------------------------------------|-------------------------------------|-------------------------------------|-----------------------|-------------------------------|
| 1,000 | 532 | 212 | 320 | 0.35 | 0.34 | 182 |
| 1,200 | 562 | 202 | 360 | 0.36 | 0.35 | 198 |
| 1,500 | 624 | 193 | 431 | 0.37 | 0.35 | 220 |

| Flow (cfs) | Total Inundated Area (acres) | Inundated Area < 1 ft Depth (acres) | Inundated Area > 1 ft Depth (acres) | Fraction Hydraulically Suitable (-) | Fraction Suitable (-) | Suitable Habitat Area (acres) |
|------------|------------------------------|-------------------------------------|-------------------------------------|-------------------------------------|-----------------------|-------------------------------|
| 1,815 | 670 | 187 | 483 | 0.35 | 0.33 | 223 |
| 2,000 | 725 | 219 | 506 | 0.33 | 0.31 | 223 |
| 2,180 | 784 | 259 | 525 | 0.31 | 0.29 | 225 |
| 2,500 | 999 | 436 | 562 | 0.27 | 0.24 | 243 |
| 3,000 | 1194 | 549 | 645 | 0.27 | 0.22 | 268 |
| 3,500 | 1338 | 631 | 707 | 0.28 | 0.22 | 291 |
| 4,000 | 1419 | 612 | 807 | 0.30 | 0.23 | 325 |
| 4,500 | 1532 | 646 | 886 | 0.31 | 0.24 | 362 |

Table C-12.—Estimated Inundation in the Compact Bypass under Option 2

| Flow (cfs) | Total Inundated Area in Bypass (acres) |
|------------|--|
| 1,000 | 25 |
| 1,500 | 44 |
| 2,000 | 51 |
| 2,500 | 60 |
| 3,000 | 70 |
| 3,500 | 84 |
| 4,000 | 98 |
| 4,500 | 112 |

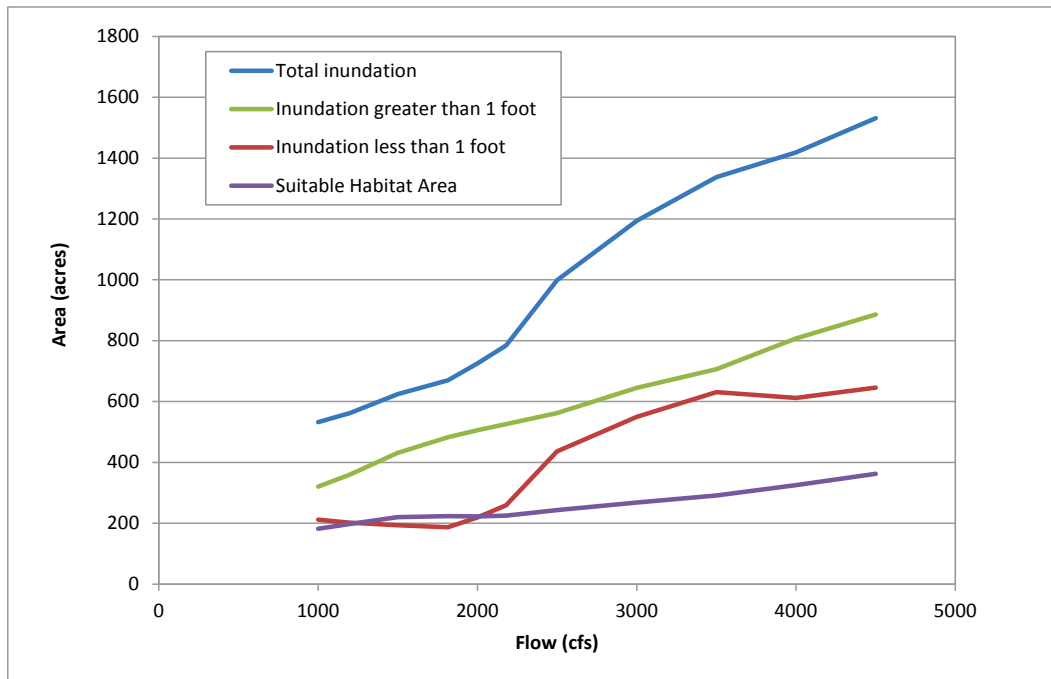


Figure C-41.—Area of inundation in Reach 2B at various flows assuming Option 2 and proposed levee alignment.



Figure C-42.—Depth of inundation for a flow of 1,200 cfs in Reach 2B under Option 2.

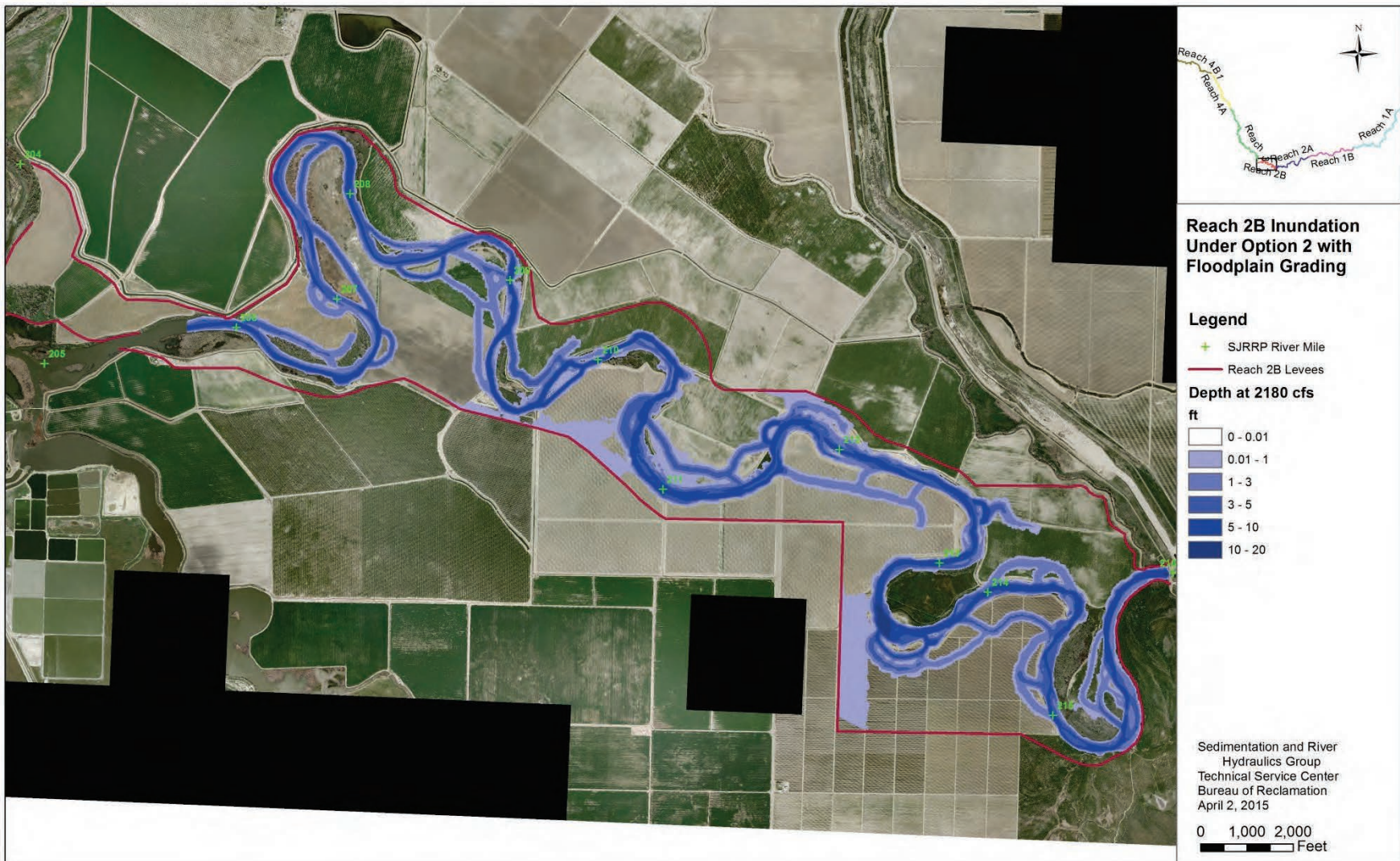


Figure C-43.—Depth of inundation for a flow of 2180 cfs in Reach 2B under Option 2.

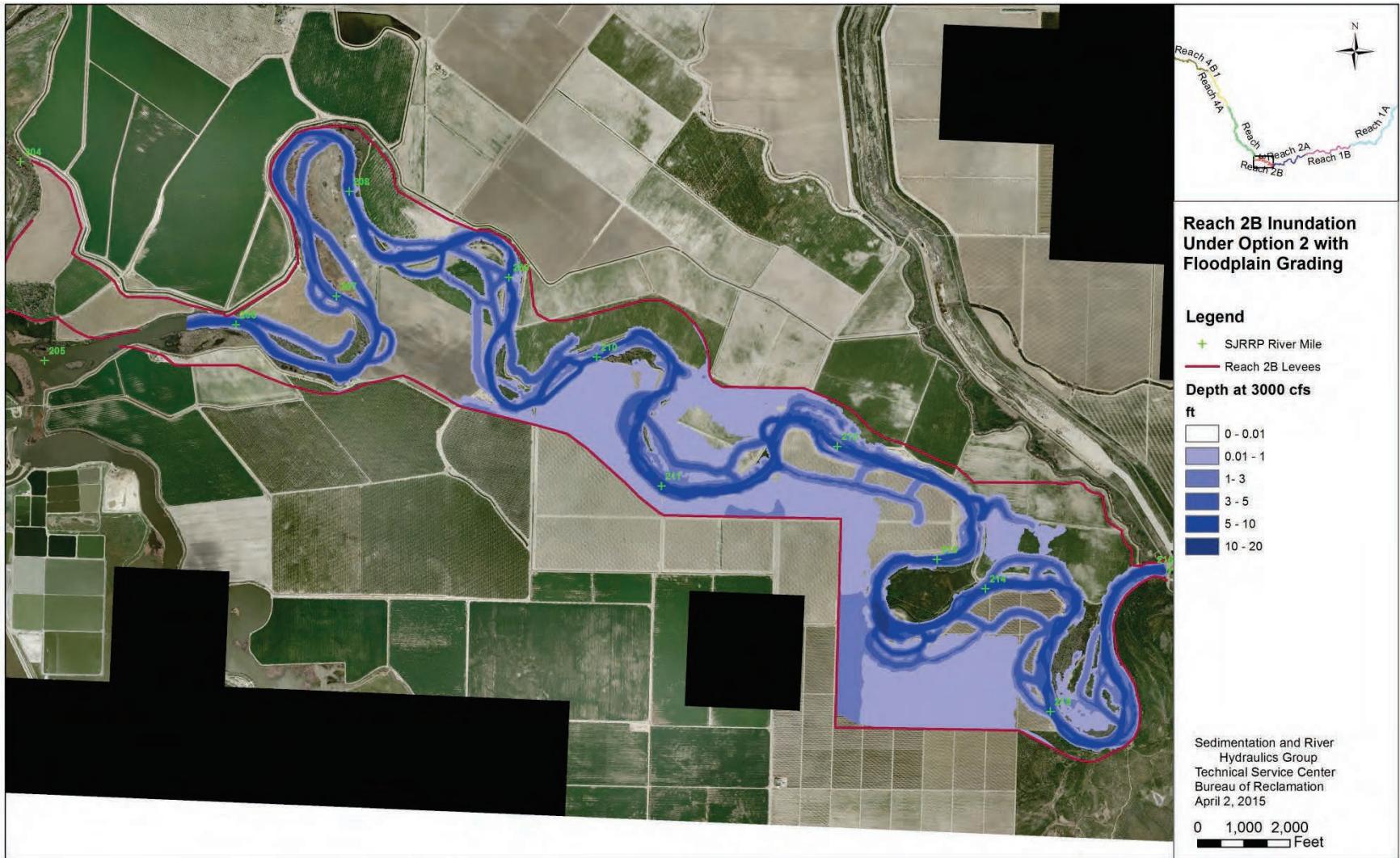


Figure C-44.—Depth of inundation for a flow of 3,000 cfs in Reach 2B under Option 2.

C.10 Impacts to Flood Conveyance in Reach 3

Both Options 1 and 2 cause significant deposition in Reach 3 immediately below the Bypass that gradually decreases to zero deposition approximately 1 mile downstream of the Bypass to RM 203. The potential length of deposition increases to 2 miles assuming no inflow from Fresno Slough. Even though there is deposition in the upper portion of Reach 3, the water surfaces at high flows are expected to decrease because of the erosion in Reach 3 over the long term.

There is, however, uncertainty in the sediment transport simulations and it is possible that erosion in the lower portion of Reach 3 does not occur. To account for this uncertainty, it was assumed that no erosion of the bed occurs in Reach 3 to estimate the maximum potential rise in water surfaces due to deposition in Reach 3. It was assumed that the deposition occurs in the first mile downstream of the Bypass (specifically from river station 448383 to 452725 in the HEC-RAS model or from RM 203.2 to 204.1). The Manning's roughness coefficients are assumed to be the same as in Tetra Tech[(2013)].

Including deposition in cross sections downstream of 448383 actually decreased the water surface elevations because in some cases there was a deposition in the lower part of the channel, but the cross section widened due to the increased flows. Therefore, the case presented in this section is considered the maximum potential rise in water surface elevations given the sediment simulations performed to date.

The maximum computed increase in water surface elevations at a flow of 4,500 cfs is 0.25 ft for Option 2 and 0.23 ft for Option 1 (figure C-45). Even with the increased water surface elevations, there is at least 3 ft of freeboard for the entire area impacted by deposition in Reach 3.

The relatively small increase in water surface elevation is due to three factors:

- 1) The average depth of flow in Reach 3 is large relative to the deposition thicknesses. Recall from Manning's equation that the mechanism for the rise in water surface is that the flow depth decreases and increases the flow velocity. The increase in flow velocity increases the friction slope which increases the water surface, but this is a gradual process and there is no sudden rise in water surface due to a relatively small change in flow depth.
- 2) The higher flows in Reach 3 also tend to widen some cross sections even in cross sections where the minimum bed elevation is increased. The overall effect is that there is only a minimal change to the conveyance.
- 3) The existing river bed in Reach 3 actually has an inverse slope for the first mile downstream of the Bypass. Therefore, even though there is several feet of deposition, the average flow depth in the impacted reach is similar to the downstream reaches.

There has been no calibration or validation of the sediment transport model for this section of the SJR. Mobile bed sediment transport simulations are subject to many types of uncertainty:

- Uncertainty of model inputs such as bed material, sediment loads, and flows.
- Uncertainty in model parameters such as channel roughness, sediment transport formula, and active layer thickness.

Given the uncertainty in sediment transport calculations, it is recommended that at this conceptual level of design, some flood mitigation is assumed to be necessary for Options 1 and 2. The most important consideration at this level of design is that there is an insignificant difference in the impact to flood conveyance between Options 1 and 2.

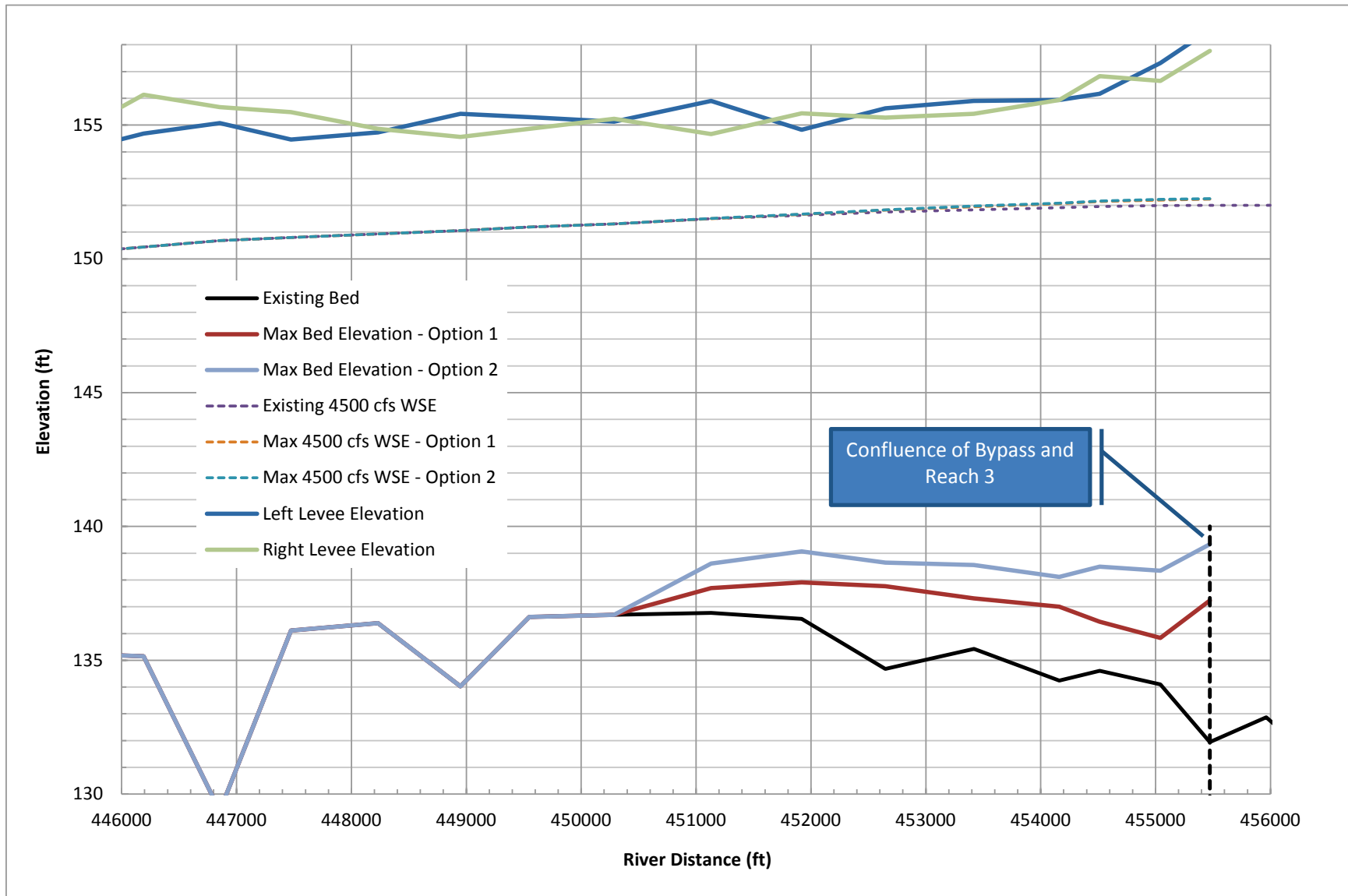


Figure C-45.—Maximum water surface elevations for a flow of 4500 cfs in Reach 3 downstream of Bypass.